Investigation of Dielectric Properties of $Ni(CuAg)Fe_2O_4$/Graphene Nanocomposite

By

Fatima Ishtiaq

School of Chemical and Materials Engineering (SCME)

National University of Science and Technology (NUST)

2019

Investigation of Dielectric Properties of $Ni(CuAg)Fe_2O_4$/Graphene Nanocomposite

Name: Fatima Ishtiaq

Reg. No: 00000172794

This thesis is submitted as a partial fulfilment of the requirement for the degree of MS in Nano science and Engineering

Supervisor: Dr. Iftikhar Hussain Gul

School of Chemical and Materials Engineering (SCME)

National University of Science and Technology (NUST)

H-12 Islamabad, Pakistan

January, 2019

Certificate

This is to certify that work in this thesis has been carried out by **Miss Fatima Ishtiaq** and completed under my supervision at the School of Chemical and Materials Engineering, National University of Sciences and Technology, H-12, Islamabad, Pakistan.

Supervisor**:** _____

Dr. Iftikhar Hussain Gul

Materials Engineering, Department
National University of Sciences and
Technology, Islamabad

Submitted through

Prof. Dr. Arshad Hussain

Principal/Dean,

School of Chemical and Materials Engineering Department

National University of Sciences and Technology, Islamabad

Dedication

I would like to dedicate this thesis to my family; the symbol of love and giving, my friends, who encourage and support me and my supervisor, who has been a constant source of knowledge and inspiration. I couldn't be able to achieve this milestone without them. This work is sign of my love to them.

Acknowledgements

‘‘ Praise is to the One, the Almighty, the merciful and the beneficent Allah, who is the source of all knowledge and wisdom, taught us what we knew not’’.

We offer our humblest thank to the holy Prophet (Peace be upon him) who is forever a model of guidance and knowledge for humanity.

It is myprivileged to express appreciation and gratitude to my research supervisor Dr. Iftikhar Hussain Gul and my committee members Dr. Zakir Hussain and Dr. Nasir Mehmood for their constant support, advice, valuable comments and efficient supervision at every stage of research work. Without their support, this could not have been possible.

I acknowledge Dr. Mohammad Arshad Hussain (Principal, SCME), all faculty members, lab engineers, lab technical staff and non-teaching staff.

I am also grateful to my family, all my friends and colleagues for giving me encouragement, appreciation and help in completing this project

Sincerely,

Fatima Ishtiaq

Abstract

In this study, a novel nanocomposite for the improvement of dielectric properties was prepared. Nickel ferrite was synthesized successfully using chemical wet Co-precipitation route. The synthesized nanocomposite is of nickel ferrite $Ni_{1-x}(CuAg)_xFe_2O_4$ doped with silver ions and copper ions (where x= 0,0.25,0.5) and decorated on graphene nano sheets using dispersive method. The $Ni_{0.5}(CuAg)_{0.5}Fe_2O_4$@Graphene nanocomposite is used for the first time to improve dielectric properties. It has been demonstrated that $Ni_{0.5}(CuAg)_{0.5}Fe_2O_4$@Graphene nanocomposite has better dielectric constant as compared to nickel ferrite.

Various techniques have been used to characterize the doped nanoparticles and nanocomposites mainly Scanning electron microscopy (SEM), X-Ray diffraction (XRD), Fourier Transform Infrared spectroscopy (FTIR) and Impedance analyser. XRD pattern of the prepared nanoparticles show that all the samples show a single phase cubic spinel structure without any impurity. XRD of nanocomposites show that there is no structural changes observed with the addition of graphene. SEM images reveal that prepared nanoparticles are spherical in shape and no agglomeration was observed. SEM images of nanocomposites clearly show that ferrites nanoparticles were homogenously decorated along the surface of the graphene sheets. Impedance analyser was used to investigate the dielectric properties of $Ni_{1-x}(CuAg)_xFe_2O_4$ nanoparticles and nanocomposites. It was observed that dielectric constant, dielectric loss, tangent loss and AC conductivity increases in doped nanoparticles due to the increase in number of the charge carriers. Graphene nanocomposites show further enhancement in all the dielectric properties due to the conductive nature of graphene. Impedance of the doped nanoparticles was also decreases because doping of copper and silver promotes the hopping mechanism of electrons. Graphene nanocomposites show further decrease in impedance values as graphene provides conductive network near the grain boundaries which ensures the fast and sustained transportation of electrons.

Table of Contents

Chapter 1

Chapter 2

Chapter 3

Chapter 4

List of Figures

List of Tables

List of Abbreviations

XRD	X-Ray diffraction
SEM	Scanning Electron Microscopy
FTIR	Fourier Transform Infrared
Ni	Nickel
Cu	Copper
Ag	Silver
P_x	X-Ray density
ρ_m	Measured density
ϵ'	Dielectric constant.
ε"	Dielectric loss
F	Force constant

Chapter 1

Introduction

Ferrites are the important class of magnetic materials that exhibit electrical and magnetic properties. The main constituents of ferrites are iron oxides and metal oxides. Ferrites have wide range of applications in transformers, sensors, inductor, green anode materials and drug delivery. Due to the advancement in Nanotechnology Nano sized ferrites have been prepared using different methods like coprecipitation, hydrothermal, sol-gel etc. Nano sized ferrites exhibit interesting and novel properties to that of their bulk ferrites. Which make them suitable for wide range of innovative applications.

1.1 History of Ferrites

The history of ferrites and their importance has been known to mankind for several centuries ago. During 470 B.C, Lodestones was discovered a specific type of rocks that had an ability to attract iron. During 12^{th} century Chinese used Lodestones in compass for navigation purpose. In 1820 Hans Christian Oersted observed that a current carrying wire caused the deflection of the compass needle which means due to the movement of charge particle magnetic field will produced. In 1825 electromagnet was invented and the fact behind the invention was that magnetic field can be produced by electric current. In 1895 Curie law was introduced which is stated that in paramagnetic materials magnetization is directly proportional to applied magnetic field. Later in 1920s the physics of magnetism was introduced with different theories regarding electrons spin and exchange interactions. In 1948 Neel theory of ferrimagnetism introduced the theoretical understanding of magnetic materials [1].

1.2 Origin of Magnetism

Everything in the universe is made up of matter and atom is the fundamental unit of matter. Atom is composed of subatomic particles named Electron, Proton and Neutron. Protons and

Neutrons present inside the nucleus, whereas electron carry negative charge revolve around the nucleus. Magnetism is the type of force which is generated in matter due to the motion of electrons. Electrons exhibit two types of motion. Orbital motion is the motion of electron around the nucleus in an orbit, this motion is very similar to the motion of planets around the sun. The other type of the motion of electron is spin motion, spinning of electron around its own axis similar to the rotation of earth around it axis. These two motions of electron cause separate magnetic moments and contributes towards the phenomena of magnetism. Magnetic moment is basically the property which interact with the applied magnetic field to produce mechanical moment. It measures the material's tendency to align with an applied magnetic field. Because of the Pauli Exclusion principle in some elements magnetic moment cancel out. According to the Pauli Exclusion principle each orbital can contain only two electrons of opposite spin. In most of the transition elements like Cobalt, Nickel, Iron magnetic moment is not cancel out and they are considered as magnetic materials.

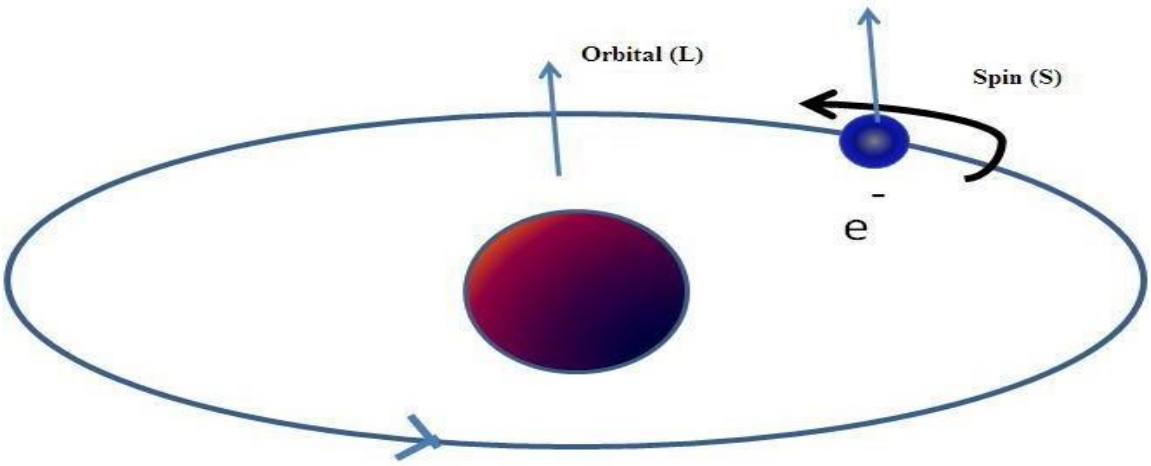

Figure 1.1. Origin of Magnetism[1]

1.3 Classification of Magnetic materials

Different materials exhibit different magnetic properties. Materials can be classified into paramagnetic, Diamagnetic, ferromagnetic and ferrimagnetic. This Classification is based on that how material respond to the external applied magnetic field, how magnetic moment behave

under the influence of applied magnetic field. Following are the different magnetic behaviours of magnetic materials.

1.3.1 Para magnetism

Paramagnetic response arises due to the presence of unpaired electrons. These materials have net magnetic moment due to the unpaired electrons. When the magnetic field is absent, dipoles are randomly arranged in domains, and their net magnetization is zero. In the presence of magnetic field dipoles align in the direction of applied magnetic field and results in the net magnetization.

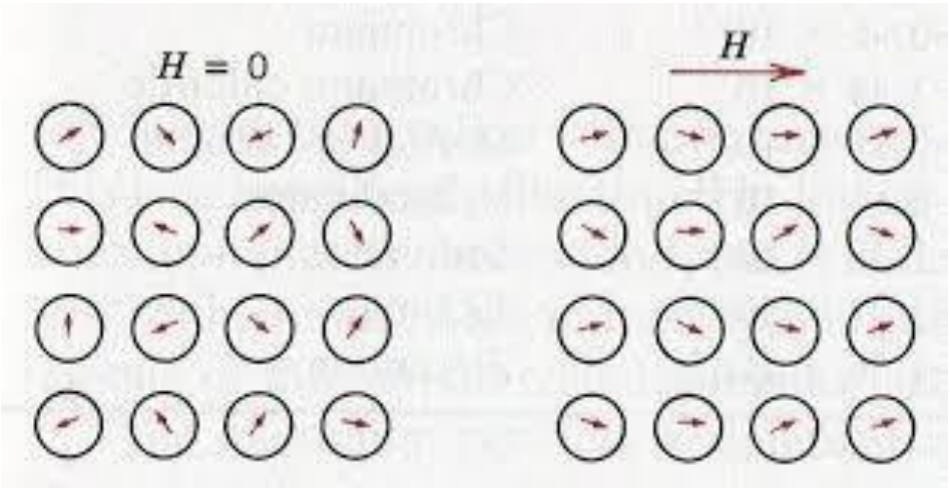

Figure 1.2. Paramagnetic material [2]

1.3.2 Diamagnetism

Materials having diamagnetic behaviour means they are repelled by the magnet. The atomic orbitals of these materials are filled, and they have no unpaired electrons. In the presence of magnetic field, weak magnetization is created in the opposite direction of the applied magnetic field, and when the magnetic field is removed there is no magnetization. These materials have negative magnetic susceptibility.

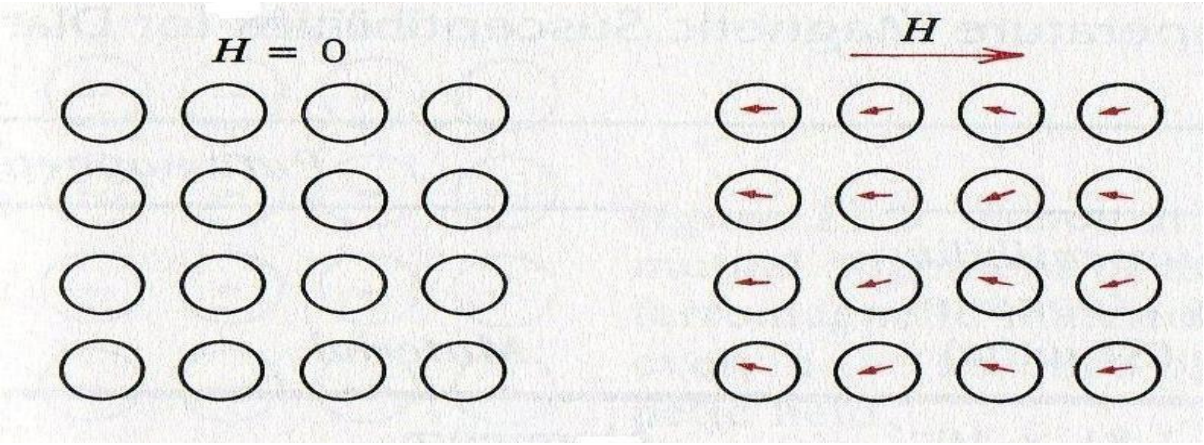

Figure 1.3. Diamagnetic material [2]

1.3.3 Ferromagnetism

Materials having ferromagnetism means they are strongly attracted by magnet. They show the permanent magnetic properties. They have unpaired electrons which are line-up with each other in a region named as domains. In the absence of magnetic field these do mains are randomly align but when the magnetic field is applied, domains arrange themselves in the direction of the applied magnetic field and when magnetic field is removed, these materials retain their magnetization behaviour to some extent.

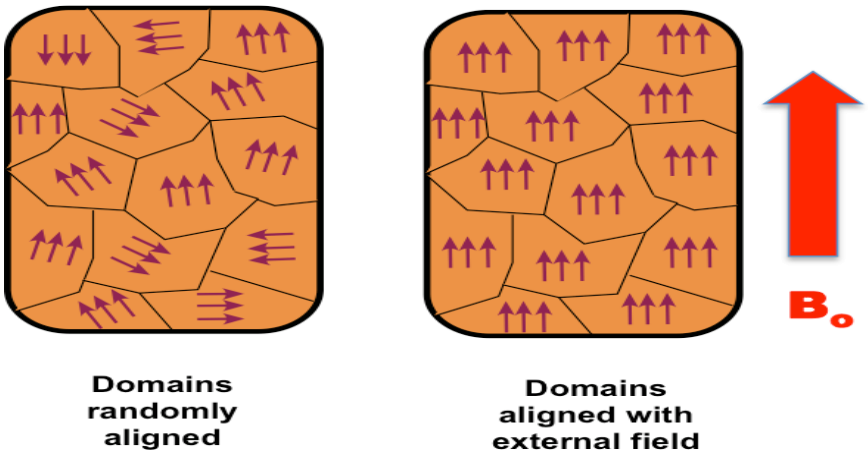

Figure 1.4. Ferromagnetic materials[2]

1.3.4 Ferrimagnetism

It is like the ferromagnetism. In these materials atoms have opposing and unequal magnetic moment, which are not completely cancel out, so these materials have some net magnetic moment. Like ferromagnetic materials, domains align in the presence of magnetic field and they also does not lose magnetic behaviour in the absence of magnetic field.

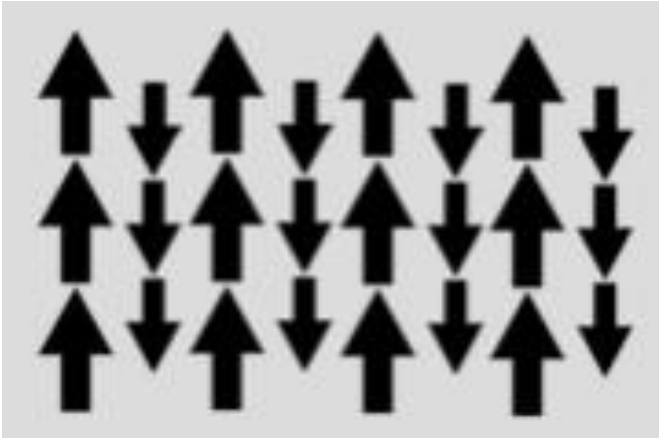

Figure 1.5. Ferrimagnetic material[2]

1.3.5 Anti-Ferromagnetism

In this type of response electron spin align with its neighbouring electrons but in opposite direction. These materials have electron spins which are equal but opposite in direction so the net magnetic moment in these materials is zero. This type of behaviour can be converted into paramagnetic behaviour above a certain temperature. This temperature is known as Neel temperature.

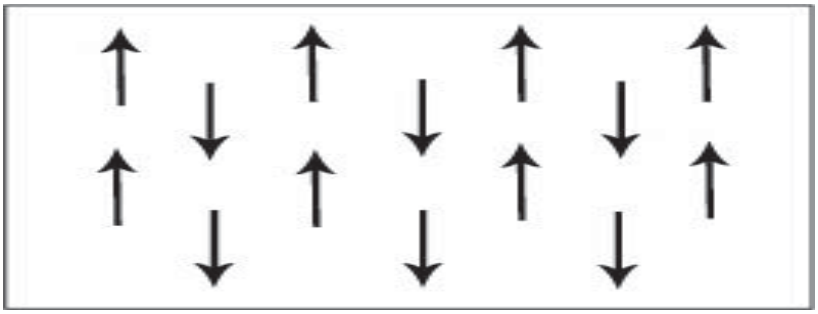

Figure 1.6. Anti-ferromagnetic material[2]

1.4 Classification of ferrites

Based on magnetic properties ferrites can be classified into two types

- Hard Ferrites
- Soft Ferrite

1.4.1 Hard Ferrites

Hard ferrites are also known as permanent magnets. As the name indicate it is really hard to demagnetize these materials once they become magnetized in the presence of magnetic field. They have high values of magnetic permeability and coercivity. Synthesis of hard ferrites require less expensive materials, and these materials are easily available. Synthesis routes of hard ferrites are cost effective which make them suitable for wide range of applications. Barium and Strontium ferrites are the common examples of hard ferrites [2].

1.4.2 Soft Ferrites

Soft ferrites are different from the hard ferrites. As the name indicates it is easy to demagnetize these materials once they become magnetized in the presence of magnetic field. They have small value of coercivity. They also have low power losses, high curie temperature and high

magnetic saturation which make them suitable for power electronic applications. Zinc and nickel ferrites are common examples of soft ferrites[3].

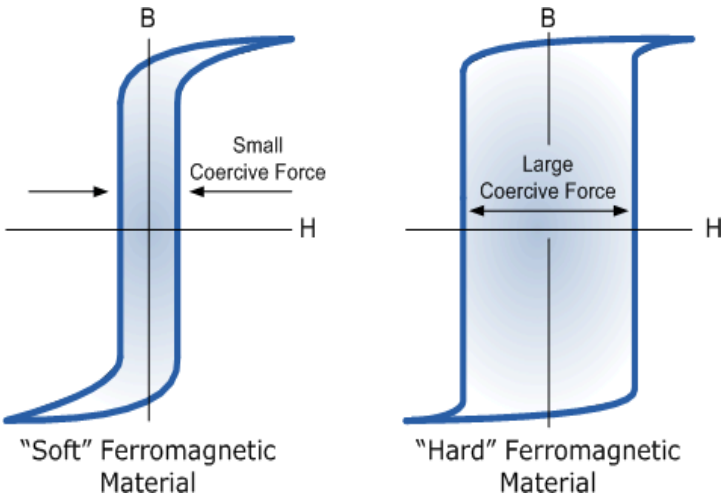

Figure 1.7. Soft and Hard magnetic material[3]

Based on crystal structure ferrites are grouped into three types.

- Hexagonal Ferrites
- Garnet Ferrites
- Spinel Ferrites

1.4.3 Hexagonal Ferrites

This type of ferrites was first identified in 1952. As the name indicate, these ferrites have hexagonal structure having formula $MFe_{12}O_{19.}$ Where M denotes an element like Barium, Strontium. The crystal structure of Hexagonal ferrites is complex in which oxygen ions arranged in a closed way to form a hexagonal structure. They show the ferrimagnetic behaviour. Due to their high coercivity they are used as a permanent magnet. They are also suitable for high frequency applications [4].

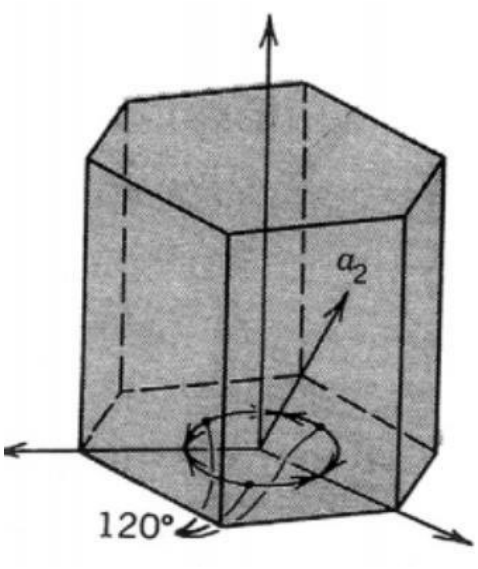

Figure 1.8. Hexagonal crystal structure[4]

1.4.4 Garnet ferrites

This type of ferrites was identified in 1957.They are represented by a formula $M_3Fe_5O_{12.}$ Where M denotes the yttrium and trivalent cation of rare earth metal. The crystal structure of garnet ferrites is developed from the garnet minerals $Mn_3Al_2Si_3O_{12}$, where Mn and Si can be replace by yttrium and Aluminium. They are also considered as hard ferrites [5].

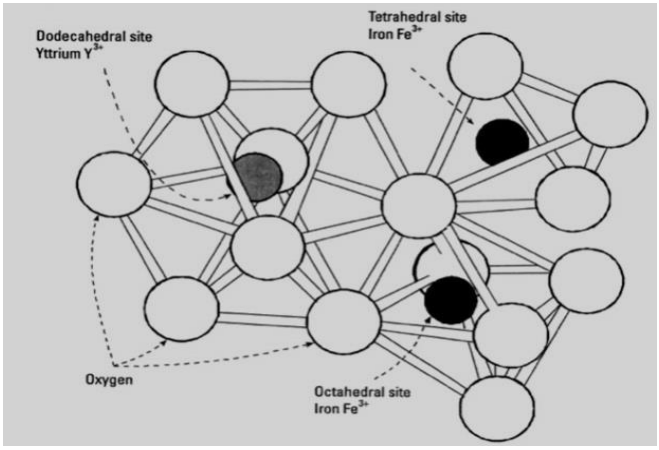

Figure 1.9. Crystal structure of garnet ferrites[5]

1.4.5 Spinel ferrites

Most widely used ferrites are spinel ferrites, they are also known as cubic ferrites. They are first identified in 1951. The chemical formula of these ferrites is MFe_2O_4, where M denotes divalent cations, examples of divalent cations are copper (Cu^{2+}), magnesium (Mg^{2+}), nickel (Ni^{2+}), cobalt (Co^{2+}), manganese (Mn^{2+}) and zinc (Zn^{2+}).The crystal structure of spinel ferrites is relatively simple than other types of ferrites. Spinel ferrites exhibit face centred cubic crystal structure where 32 oxygen atoms are present. Cations occupy two different sites and these sites named as tetrahedral and octahedral sites. There are total 64 tetrahedral sites out of which 8 sites occupied with metals similarly number of octahedral sites are 32 out of which 16 sites occupied by anions [5].

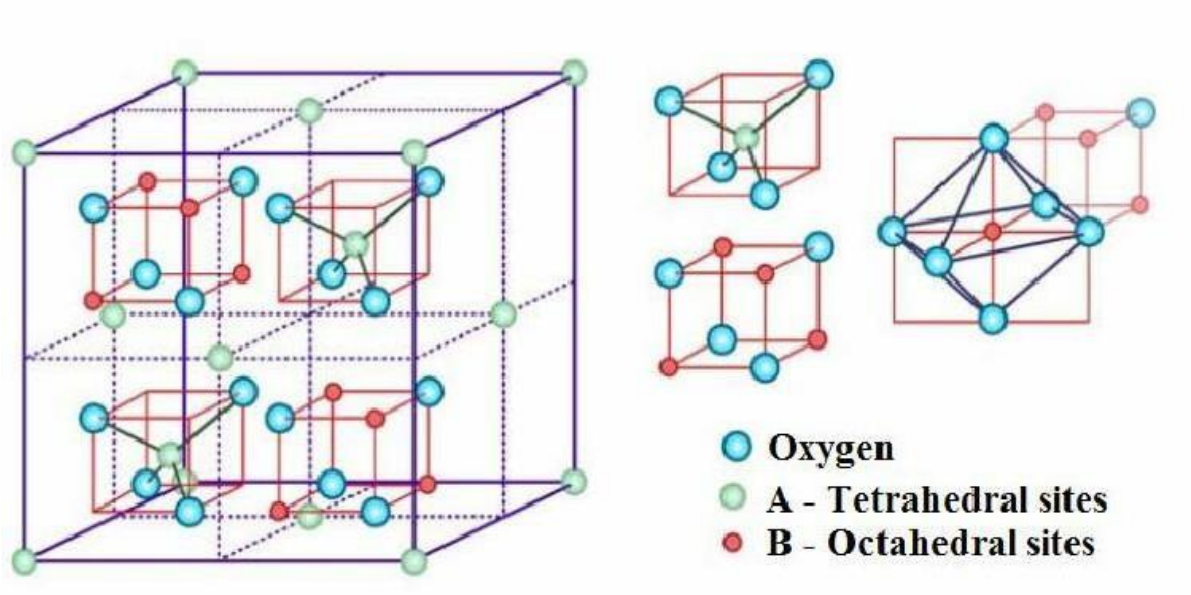

Figure 1.10. Spinel ferrites unit cell showing tetrahedral and octahedral sites[5]

Based on cations distribution spinal ferrites can be classified into three types.

- Norma spinel Ferrites
- Inverse spinel Ferrites

1.4.5.1 Normal spinel Ferrites

In normal spinel ferrites divalent cations occupy tetrahedral sites while octahedral sites are occupied by trivalent cations. Example of normal ferrite is zinc ferrites.

1.4.5.2 Inverse spinel Ferrites

In this type of ferrites divalent cation occupy octahedral sites while trivalent ion distributed in both tetrahedral and octahedral sites. Example of inverse ferrite is nickel ferrite.

1.5. Nickel Ferrite

Nickel ferrites is considered as a most widely used spinel ferrite regarding power electronic industry, because of its high values of saturation, high Curie temperature and low power losses. Nickel ferrite possess inverse spinel structure, which is face-centered cubic structure contain 32 oxygen ions. In this crystal structure Nickel (Ni^{+2}) occupy octahedral sites and Iron(Fe^{+3}) occupy both tetrahedral and octahedral sites [6]. In the crystal structure of ferrite nature and type of the ion and their distribution on tetrahedral and octahedral sites are responsible for the unique and interesting electrical and magnetic properties. The magnetic properties arises due to the magnetic moments of cations on tetrahedral and octahedral sites. The nickel ferrites nanoparticles show the superparamagnetic behaviour having zero remanence and zero coercivity. The value of saturation magnetization is small for ferrite nanoparticles as compared to their bulk form due to the large surface to volume ration and core shell morphology [7].

Nickel Ferrites nanoparticles can be prepared by different synthesis routes. Arrangement of cations in crystal structure and properties of nickel ferrites nanoparticles strongly affected by synthesis approach. Physical and Chemicals methods are used for the preparation of ferrites nanoparticles, physical method include mechanical ball milling and inert gas condensation. Chemical methods are more often used for the preparation of ferrites nanoparticles because of their low cost. Most common methods which are used for synthesis of nickel ferrites nanoparticles are co precipitation, hydrothermal, reverse micelle and sol gel [6].

1.6 Concept of doping in Ferrites Nanoparticles

Doping is the common approach in which an impurity, an atom or ion intentionally introduce into the crystal structure of ferrites to alter the different properties of ferrites nanoparticles. Electrical and magnetic properties of ferrites depend on the cations distribution within the crystal structure. Dopant ion and atom has different ionic radii, which affects the lattice parameter of whole crystal structure, similarly dopant ion and atom has different magnetic moments which changes the magnetic response of parent crystal structure. Different dopants like Cu^{2+},Co^{2+},Mn^{2+},Mg^{2+} and Zn^{2+} introduced into the crystal structure of nickel ferrites nanoparticles to modify the properties, Moreover trivalent cations Nd^{3+},Al^{3+}can also bi introduced into the system as a dopant.

1.7 Applications of Ferrites

Ferrites have important and unique properties which make them suitable for wide range of applications. The main properties of ferrites include, High magnetic permeability, high electrical resistance. Ferrites are considered as a good magnetic material as compared to pure metals because of their easy and low-cost manufacturing. Their high magnetic permeability is useful for devices e.g. antennas. Their high electrical resistance is useful for transformer to reduce eddy currents [8].

Following are the applications of Ferrites:

- Inductor: Ferrites are considered as an important inductive component for electronic circuit devices e.g. filters, amplifiers.
- Magnetic sensors. Ferrites having piezoelectric oxides considered as a new generation of sensors. Magnetic sensors have ability to convert the magnetic field into electrical signals. The basis of this mechanism is that due to the magnetic field mechanical strain is produces on the ferrites because of their magnetostriction and after that strain produces an electrical signal in piezoelectric layers.
- High frequency applications. Application of high frequencies includes telecommunications and radar system. Because of the non-conductive nature of ferrites, they allow the complete penetration of electromagnetic field as compared to the metals

because in metals skin effect limit the complete penetration of high frequency electromagnetic fields.

- Power applications. Ferrites are useful regarding power supplies for variety of devices e.g. TV, video and computer systems. In switch mode power supplies ferrite transformers are used to rectify the signals so that instrument receive the required power.
- Biomedical applications. Magnetic nanoparticles are extremely useful regarding biomedical applications. Ferrites are used for the detection, modification and study of human cell. The important application of ferrites in this field is hyperthermia, in which thermal energy which comes from hysteresis loss of ferrites used in the treatment of cancer cells.
- D.C applications. Hard ferrites which are used as a permanent magnetic are suitable for loudspeakers, D.C motors, microphones and in other portable devices.

Figure 1.11. Applications of Ferrites[8]

1.8. Introduction of Graphene

Graphene is considered as a wonder material of 21st century. Graphene is the stable allotropic form of carbon. It is a two-dimensional structure having sp2 carbon atoms which are arranged in a honeycomb lattice to form thin layers. Graphene exhibits the ordered structure because there is strong bonding present between adjacent carbon atoms. Carbon is non-metal, but the conductivity of graphene is varying between conductors or insulators so graphene act like a semi metal. Basically, the delocalization of bonding electrons throughout the 2D lattice structure responsible for the unique properties of graphene. It is considered as a strongest material, the tensile strength of graphene is approximately 130 GPa, which is much higher than the steel. Graphene also exhibit elastic properties, having high Young's modulus of 500GPa. High electron mobility of graphene is due to conjugated π-electrons, these electrons considered as a massless particles and they travel without any type of scattering and responsible for the high carrier mobility of graphene [9]

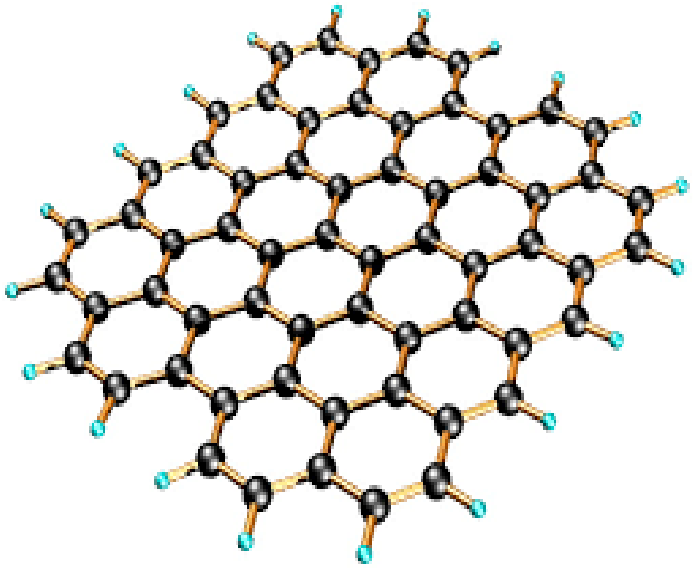

Figure 1.12. Thin layer of Graphene[9]

Synthesis of graphene include both top down and bottom up approaches. Following are some methods to produce graphene.

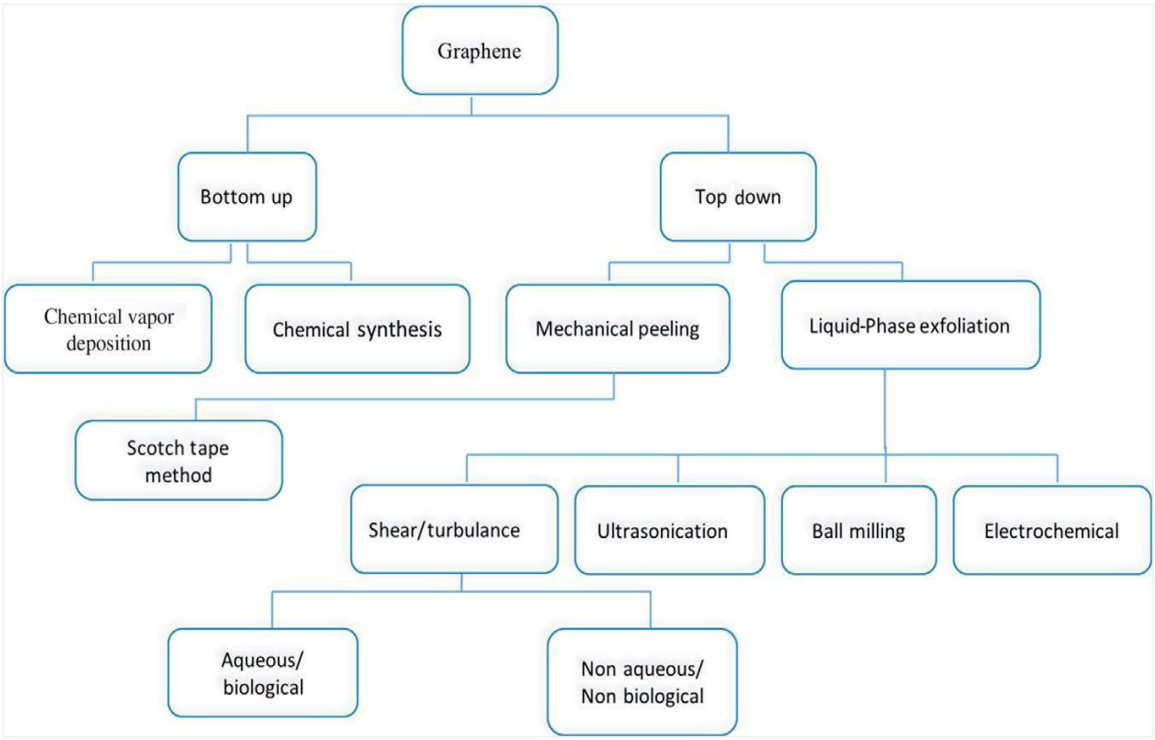

Figure 1.13. Synthesis routes of Graphene[9]

1.9 Applications of the Graphene

Due to the unique properties of graphene it can be used as [10].

- Transistors
- Frequency multiplier
- Sensors
- Transparent conducting electrodes
- Optical modulator
- Energy storage device
- Catalyst
- Water proof coatings
- Radio wave absorber
- Biomicrorobotics

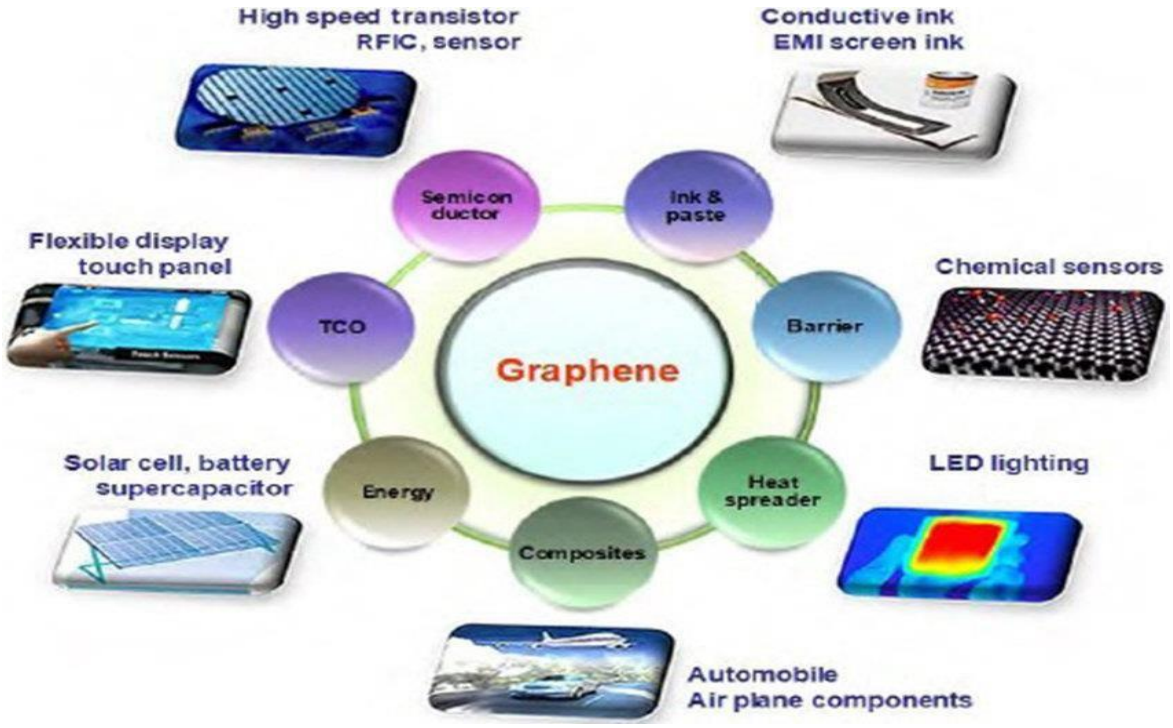

Figure 1.11. Applications of Graphene[10]

1.10 Aims and Objectives

The objectives of this research work are as follows:

- Using a simple, effective and inexpensive Co-precipitation route for the synthesis of copper silver doped nickel ferrites nanoparticles.
- Synthesis of prepared doped nickel ferrites nanoparticles and graphene nano composites using dispersion method.
- Study the effect of dopants and graphene on nickel ferrites nanoparticles and investigate their dielectric properties.

Chapter 2

Literature Review

Dong-Hwang Chen et al. prepared nickel ferrites nanoparticles by sol gel method. In this synthesis polyacrylic acid (PAA) used as a chelating agent. They used various ratio of PAA and calcine the sample at 300° C for 2 hours. It is observed that by varying the molar ratio of PAA and the calcination temperature, the diameter, surface area and crystallinity of the prepared nanoparticles could be controlled. Prepared nickel ferrites nanoparticles have diameter of 5 to 30 nm, and they have specific surface area of 20.0 to 55.2 $\frac{m^2}{g}$. They also studied magnetic properties of prepared nickel ferrites nanoparticles and results showed the superparamagnetic behaviour of particles. The value of their saturation magnetization is 0.19 emu/mol at 298 K [11].

YuanLiu et al. prepared nickel ferrites nanoparticles by sol gel method. In this synthesis citric acid is used as chelating agent. Its structural and microwave absorption properties were studied by X-ray diffraction and network analyser. Morphology of prepared nickel ferrites nanoparticles were analysed by scanning electron microscope. Results indicate as the concentration of citric acid increases particles size first increases and then decreases, best ratio of citric acid that used for the synthesis of nanoparticles with metal ion is nCA: nFe: nNi =4:2:1.Calcination temperature effects the microwave absorption properties of prepared nickel ferrites nanoparticles, increase in calcination temperature improves the microwave absorption properties [12].

Pathan Amjadkhan et al. studied dielectric properties and ac conductivity of nickel ferrite nanoparticles. Nanoparticles were synthesized by sol gel method. The calcination temperature was 600° C. Structural properties were analysed by X-ray diffraction which shows that change in XRD pattern is due to the shifting of ions between tetrahedral and octahedral sites. Dielectric

properties of the prepared samples have been carried out using impedance spectroscopy. The high value of dielectric constant is associated with the structural changes of prepared nickel ferrites nanoparticles. The conductivity of the prepared samples increases with increases in frequency. Nanoparticles of nickel ferrites shows AC conductivity of $1.0 * 10^{-4}$ $\frac{S}{cm}$, this is associated with the dipole polarization of prepared samples [13].

Vithal Vinayak et al. prepared nickel ferrites nanoparticles by using coprecipitation method. X-ray diffraction confirm the formation of single cubic structure of nickel ferrites. Lattice constant of synthesize nanoparticles was calculated from XRD pattern which is 8.232Å. The crystallite size obtained from XRD pattern is 37nm.Microstructure analysis from scanning electron microscopic images shows the grain in nanometre range. The magnetic properties of prepared nickel ferrites nanoparticles were investigated by using pulse field hysteresis loop technique. Magnetic parameters like values of saturation magnetization, remanence magnetization and coercivity were calculated from obtain hysteresis loop of nickel ferrite nanoparticles. Which shows the ferrimagnetic behaviour of nanoparticles [14].

Safia Anjum et al. prepared Copper doped nickel ferrites nanoparticles by double sintering method and studied their structural, dielectric and magnetic properties. X-ray diffraction and scanning electron microscopy used to investigate the structural properties. With the increase in copper concentration lattice parameter is also increases. This is since copper having a large ionic radius as compared to the nickel ionic radii and doped copper ion replace the nickel ion as a result lattice parameter increases. LCR meter used to investigate the dielectric measurements. Dielectric constant decreases at higher frequency. It could be explained by Maxwell and Wagner model, which is associated with the space charge polarization with in the dielectric medium [15].

K.Vijaya Babu et al. studied the structural and dielectric properties for high frequency application of mixed ferrites nanoparticles. In this work two different kind of spinel ferrites prepared by sol gel route, Copper doped nickel ferrites and cobalt doped nickel ferrites. X-ray diffraction reveal that copper and cobalt replace the nickel ion on tetrahedral site and lattice

parameter of doped ferrites nanoparticles increases because of the larger ionic radii of dopants. FTIR shows the characteristics bands of prepared ferrites and it is observed that bands are

shifted towards the low frequency side in case of dopant this is because of the cation distribution. Samples shows high dielectric constant at low frequency due to the defects and dislocation in doped ferrites crystal structure [16].

Pengfei Yin et al. studied the effect of graphene on cobalt doped nickel ferrites nanoparticles regarding microwave absorption application. Cobalt doped nickel ferrites nanoparticles were prepared by using hydrothermal method. 2D structure of graphene responsible for multiple scattering and enhance microwave absorption. Graphene based ferrites composites show the maximum reflection up to 30.92dB at 0.84GHz for 12 wt.% graphene content. Because of the excellent conductivityof graphene and large surface area, Microwave absorption properties of doped ferrites nanoparticles improved [17].

Sumair Ahmed Soomro et al. $NiFe_2O_4$/MWCNTs composites were prepared by ultrasonication method. To enhance the dielectric properties of nickel ferrites, MWCNTs used. Structural information obtained from X-ray diffraction. Porosity is increases with the addition of MWCNTs as more interface and defects formed. Scanning electron microscopy clearly shows the complete anchoring of nickel ferrites nanoparticles on MWCNTs. Dielectric measurements shows the enhancement in dielectric properties with the addition of MWCNTs, Because of conductive nature of MWCNTs and space charge polarization mechanism [18].

M.A Ahmed et al. Studied the structural and magnetic properties of silver doped nickel ferrite nanoparticles. Citrate sol gel was used for the preparation of nanoparticles. X-ray diffraction used to analyse the structure of prepared nanoparticles. It was observed secondary phases of haematite also formed due to the segregation of silver ions on grain boundaries. Moreover, lattice parameter increases due to the larger ionic radii of silver ion. Faraday's method was used to calculate the magnetic susceptibility. It was observed by increases silver ion magnetic moment decreases and it is due to the nonmagnetic characteristics of silver ions [18].

Shahida Akhter et.al Studied structural and physical properties of zinc doped copper ferrites nanoparticles, these nanoparticles prepared by using sintering ceramic method. X-ray diffraction reveals that with the addition of zinc in copper ferrites nanoparticles lattice parameter increases. Bulk and x-ray densities were also calculated from XRD pattern and it was found that with the addition of zinc bulk density decreases and porosity increases. Zinc as a dopant cause densification of material [19].

Lili zhang et al. Studied the electromagnetic absorption properties of iron oxides and graphene oxide composites. These composites were prepared by using thermochemical reactions. X-ray diffraction and Transmission electron microscopy used for the structural analysis. It was observed that composites show better electromagnetic absorption properties as compared to separate iron oxide and graphene oxide. Composites have high stability which is suitable for high temperature applications [20].

Rajinder Singh et al. Prepared the nickel ferrites and nitrogen doped graphene composites for photocatalysis application. The composites were prepared by using hydrothermal method. Scanning electron microscopy shows that nickel ferrites nanoparticles decorated on the surface of nitrogen doped graphene. The measurements of photocatalysis activity shows that, Nanoparticles bound with nitrogen doped graphene converts the inactive nickel ferrites into a better catalyst for degradation of methylene blue. The increased value of saturation magnetization and coercivity was observed for the composite [21].

Ahmet Teber et al. Prepared the Manganese and Zinc ferrites nanoparticles by using sol gel method. These prepared nanoparticles then blended with the MWCNTs in different ratios. Paraffin were used as a binder matrix. Their microwave absorption properties were studied. X-ray diffraction show no secondary phase form and additional peak of MWCNTs observed in XRD patterns. Microwave absorption properties of MWCNTs were enhanced due to the incorporation of magnetic materials. The minimum reflection loss is about 99.99% [22].

Xingchen Zhao et al. Prepared iron oxide and graphene composites by the reduction reactions and hydrothermal methods. Raman technique is used to identity the presence of graphene. Scanning electron microscopy used to analyse the microstructure of iron oxide coated graphene sheets. Microwave absorption properties shows that dielectric properties of iron oxide and graphene composites is different from the uncoated graphene sheets. Charge transfer and polarization of carriers enhance in composites which contributes towards the excellent microwave absorption properties [23].

J. Balavijayalakshmi et al. Synthesize cupper doped nickel ferrites nanoparticles by coprecipitation route and studied their dielectric properties. The XRD study confirm the formation of single cubic phase of copper doped nickel ferrites nanoparticles and particles size decreases as the concentration of cupper increases. The dielectric constant decreases for all the composition due to the formation of secondary phase [24].

E.Ranjith Kumar et al. Prepared the manganese doped copper ferrites nanoparticles by auto combustion method and studied their structural and dielectric properties. The XRD pattern reveal samples without heat treatment shows the single cubic phase of nanoparticles, but as the annealing temperature increases secondary phase formed. TEM images shows that the samples are spherical in shape and the size range is from 40 to 60 nm. Dielectric constant decreases with the increase in particle size [25].

Zhou Wang et al. Synthesized MWCNTs-epoxy composites by mechanical mixture method. The microstructure, dielectric constant and microwave absorption properties of composites investigated. The absorption properties of composites were measured between 2 to 20 GHz. The defects in MWCNTs can act as polarization centres and show better microwave absorption. Moreover, microwave absorption also depends on the loading amount of MWCNTs. SEM images reveal that MWCNTs homogenously dispersed in the epoxy matrix [26].

Jianjun Fang et al. Prepared the nickel and graphene composite by electrodeposition method and studied their microwave absorption response. SEM images reveal the porous structure of

graphene and shows nickel decorated graphene pattern shows the nickel functionalized graphene nanosheets. Microwave absorption properties shows that nickel graphene composites show better results of absorption than graphene. Nickel is densely coated on graphene so soft magnetic and conductive properties contributes towards better microwave absorption properties [27].

Xiqing yuan et al. has done synthesis of graphene platelets and studied their application for lithium ion batteries. Graphene platelets were doped with the sulphur and nitrogen. Novel method is used for doping. L-cysteine is used as a precursor on a water-soluble salt. This water-soluble salt used as a template. There are three different nitrogen, sulphur and ammine group present in L-cystine. Carboxylic groups can be used to functionalize these groups. There is more sulphur and nitrogen sites and it is considered to possesses better conductivity. The composite of graphene nanoplatelets and sulphur shows high current density and the discharge capacity is increased. This process will enable the unique design of cathode material for the production of Li-S batteries [28].

Y.C yang et al. studied nickel ferrite and its different properties like electrical, magnetic and structural properties. Composites of the nickel ferrite with different transition metals and rare earth metal was also studies. The particles were prepared by different the methods including sol-gel method and co precipitation method. The samples prepared by sol-gel route exhibit large particle size and they have high resistivity, ferromagnetic behaviour and multi-domain. The prepared particles can be used in wide range of applications involving high frequency. The particles prepared by co precipitation method show small particle size, paramagnetic behaviour and had only single domain. The prepared particles are applicable in different medical applications like magnetic resonance imaging, drug delivery etc. when nickel ferrite is doped with different rare earth element the reduction in the magnetization is observed. The increase in coercively is observed by doping

transition metal. The decrease in dielectric loss is noticed when doped with rare earth metal ions [29].

Roul Valenzuda studied the applications of ferrites in different electronics fields. He also studied the different composites of ferrites. Now a day the electromagnetic interference arises because of the considerable increase in usage of different electronic equipment. Due to the presence of high speed digital interfaces in electronic media like computer and sensors huge rest of disturbance created. The electric field and magnetic field also causes disturbance in wireless system. This phenomenon is considered as electromagnetic interference. The electrical devices usually produce noise at different frequencies. To reduce the interference, the particles that are designed should behave like low power filters [30].

R.C. Chie at al. combines and studied carbon nanomaterial with ferrite. The prepared composite showed better microwave absorbing properties. The composite of carbon nanotube and cobalt ferrite was prepared by chemical vapor deposition in which cobalt ferrite used as a catalyst. The results showed improved microwave absorption properties. Carbon nanotubes responsible for the dielectric loss of incident electromagnetic wave and ferrites responsible for the magnetic loss of incident wave. Separately both are not good absorbers. Nano composite is the good combination of magnetic loss and dielectric loss. This will result in excellent microwave absorption [31].

Dinesh kumar et al. synthesized graphene nano platelets by using microwave assisted method. Microwave exfoliation was used for the synthesis of graphene nano platelets. The process also involved the expandable graphite. The microwaves were made to fall on the expandable graphite for three minutes. Later on sulphuric and nitric acid were used for the completion of method. The graphene nano platelets prepared by this method were analysed using the different characterization techniques. The prepared graphene nano platelets showed very high purity. There was no observed structural damage. The traces of oxides were also present. The prepared graphene nano platelets were little thick in layer, variable in size and crystalline in nature. The microwave method for producing graphene sheets is considered as effective method [32].

D.I. Zoha et al. synthesized nickel ferrite graphene composites and studied their photo catalytic properties. Polyacrylamide gel used during the synthesis and the size of the prepared samples was 31nm. The composite of ferrite and graphene was prepared by using sol gel chemical method. SEM images showed excellent adhesion of ferrite particles in graphene sheets. Methylene blue was uses for the photo catalytic activity of prepared sample. The results

showed improved photocatalytic performance as compared to simple nickel ferrite. The specie that plays an active and important role in degradation is hydroxyl radical [33].

Zehra et al. worked on graphene and its composite with hard ferrite to determine the microwave absorbing properties. Barium ferrite nanoparticles were prepared by using sol gel route. They are combining with the graphene sheets. The barium hexaferrite nanoparticles were decorated on graphene sheets. The novel and unique composite as prepared to find out its microwave absorbing properties. The barium ferrite nanoparticles embedded on graphene show increased absorption. Due to layered structure of the prepared samples the shielding activity shows much better results. The phenomena involve multiple reflections. Absorption is reason for better performance. The physical and structural properties indicates that graphene/ barium ferrite show enhanced microwave absorbing properties [34].

Christopher R. Herron used simple method to synthesize thin films of graphene. Andy Wieto et al. used spark plasma sintering method for synthesis of graphene nano platelets and studied their properties. Graphene nano platelets have ability to maintain their structure and they can also bear extreme sintering conditions. Graphene nano platelets exhibit two-dimensional structure. The synthesis of graphene nano platelets in bulk form enable to study various mechanisms directly. Knowledge of theses mechanisms help to observe the behaviour of graphene nano platelets in composites where they act as secondary phase. The structure of the prepared graphene nano platelets was corrugated. Graphene nano platelets are considered as a best reinforcing agent in ceramics. The toughness of the composite has also improved because graphene nano platelets helps to stop the propagation of cracks and defects. Synthesized graphene nano platelets improved toughness and reduced friction [35].

C. Murugesan et al. Prepared cobalt ferrites nanoparticles by using low temperature method which is auto combustion and high temperature method which is ceramic method. SEM images show different grain size of cobalt ferrites prepared from different methods. XRD pattern reveal both methods produce single cubic structure. The value of lattice parameter is higher for the sample prepared from ceramic method. FTIR is performed to investigate the tetrahedral and octahedral sites of ferrites. Cobalt ferrites prepared from auto combustion have and cobalt ferrite prepared from ceramics method have high saturation magnetization high coercivity [36]

Chapter 3

Materials and Methods

Synthesis methods of nanoparticles can be classified into two main groups.

- Top down
- Bottom up

3.1. Top down approach

As the name indicate, in this approach large piece of material cutting down to create a desire nanostructure. This approach is commonly used in electronic industries. Examples of top down approach are Lithography, Mechanical milling, skiving, molding and Ball milling [37]. In lithography technique electron, x-ray and light beam is made to fall on selective portion to create unique nanostructure pattern. On the commercial level top down approach is applicable but there are drawbacks associated to that approach.

- Limited for the Nano fabrication because of the wavelength of light and size of tools used in this approach.
- Impurity present in the prepared structures form this approach.
- Three dimensional objects are difficult to construct because top down approach involves planar techniques deal with the addition and subtraction of pattern layers.

3.2. Bottom up approach

As the name indicate, in this approach basic building blocks like small molecules and atoms assembles together to create the required nanostructure. Biological system provides the inspiration for the bottom up approach. Chemical and physical forces play important role in this approach. Common examples are sol-gel, coprecipitation and micro emulsion. There are

several advantages of bottom up approach like its includes low temperature technique which are efficient and easy to handle and cheap [38].

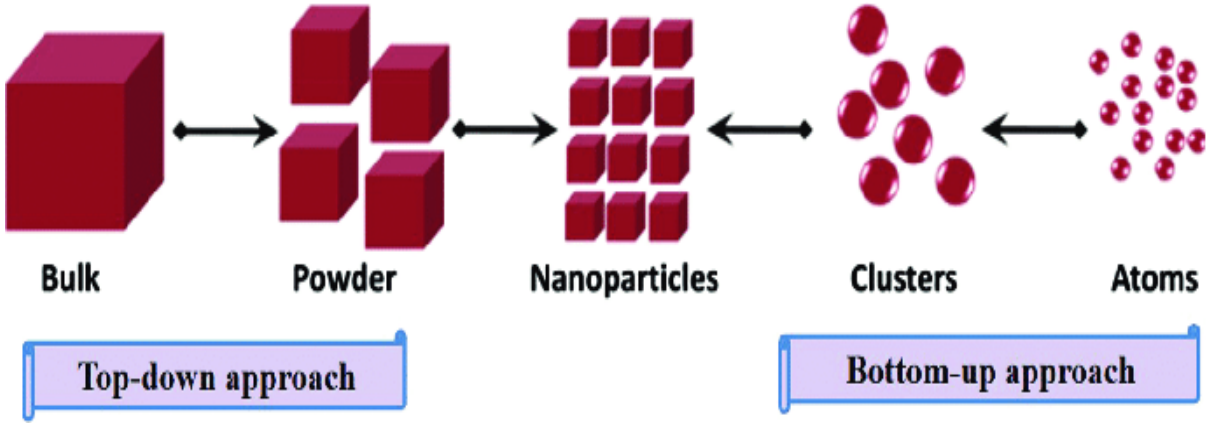

Figure 3. 1 Top down and Bottom up approach[39]

Bottom up approach includes following methods which are widely used in the synthesis of nanoparticles.

- Sol gel
- Hydrothermal
- Sono-chemical
- Micro emulsion
- Gas condensation
- Combustion flame synthesis
- Co precipitation

3.3. Sol-gel Method

Sol-gel process is considered as a versatile chemical process, which is widely used in the preparation of ceramic and metal oxides materials. This process usually uses metal alkoxides and inorganic salts as precursors. In this process hydrolysis and polycondensation take place

to prepare a colloidal suspension. This process influences the morphology of particles during chemical reactions of the precursors [39].

3.4. Hydrothermal Method

This synthesis is carried out in a specific pressurized container called auto clave. The temperature inside the autoclave can be raised above the boiling point of water. This method is useful for the particle morphology, to control grain size. Hydrothermal is used for the synthesis of metal oxides nanoparticles [39].

3.5. Chemical Co-precipitation Method

Co-precipitation is the simple and efficient method to synthesize nanoparticles. Fumes are produced during this process which is considered as a drawback, but this synthesis should be done in the fume hood to avoid the interaction of fumes with lab environment. The main steps of this process are nucleation, growth, agglomeration and coarsening. All the process occurs simultaneously. Nucleation is the initial process in which small atoms and ion arranged in a specific manner and creating a site in which additional atoms deposited and crystal grow. These newly formed crystallites are not stable thermodynamically and they aggregate to make stable. This mechanism is called growth. Coarsening is the process in which small particles combine with the large one, this is the part of growth process.

The precursors which are mostly used in Co-precipitation method for the synthesis of ferrites nanoparticles are chlorides and nitrates. All the required precursors are added into the water after that on the addition of the alkaline solution metal hydroxides form and precipitates out in water. Mostly Sodium hydroxide used as an alkaline solution, then resulting solution washed out with deionized water many time to attain neutral pH, during washing all the chlorides and nitrates washed away. Now the neutral solution dried and calcine to obtain final form of nanoparticles [40].

3.6. Advantages of Co-precipitation

Co-precipitation is the easy and low temperature method to synthesize pure and chemically homogenize ferrites nanoparticles. The size and morphology of the prepared nanoparticles is

depending on various factor of synthesis routes like pH, temperature, molarity. In Co-precipitation all these factors can be control to obtain desire size and morphology of the

prepared samples. Homogenous and monodispersed nanoparticles formed by using Co-precipitation method.

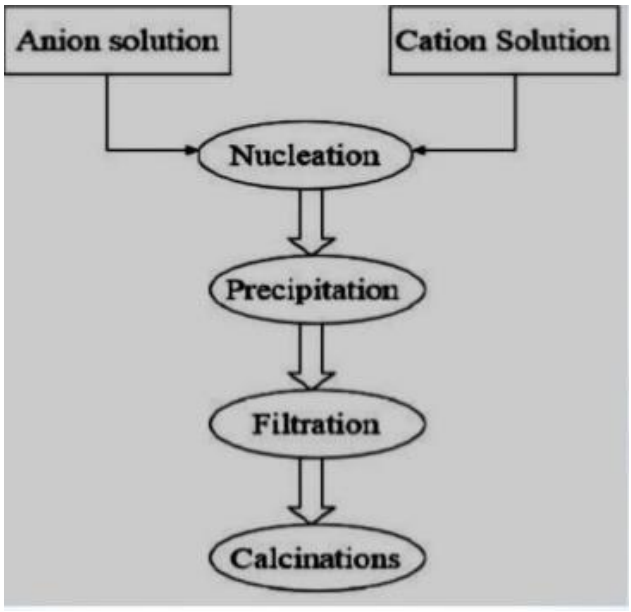

Figure 3.2. Steps involve in Co-precipitation Method[41]

3.7. Steps of Co-precipitation

Mainly two steps involved in co-precipitation method for the synthesis of nanoparticles.

- Co-precipitation step
- Ferritisation step

3.7.1. Co-precipitation step

During reaction metal ions co-precipitate in the basic medium as a result colloidal particles of metal hydroxides formed. Following will be the reaction process in the case of nickel ferrites

$$Ni(NO_3)_2.\ 6H_2O + Fe(NO_3)_3\ .\ 9H_2O + NaOH$$

$$Ni(OH)_2.\ Fe(OH)_3 + NaNO_3$$

3.7.2. Ferritisation step

Metal hydroxides obtained from Co-precipitation step is heated in alkaline medium as a result nickel ferrite nanoparticle formed.

$$Ni(OH)_2.\ Fe(OH)_3 + NaNO_3$$

$$Ni_xFe_2O_4.\ nH_2O + (4\text{-}n)\ H_2O + NaNO_3$$

3.8. Variables involves in Co-precipitation method

Following are the factors play important role during Co-precipitation method

- Role of anion
- Rate of mixing of the reactants
- Effect of pH
- Temperature effect
- Heating after Co-precipitation

3.8.1 Role of Anion

Salts and the solution use during Co-precipitation method are the sources that provide anions. Nature of anion involve during process has unique effect on the properties of prepared nanoparticles. Mostly the metal salts give the better results, this is the reason chlorides and nitrates widely use in Co-precipitation method.

3.8.2 Rate of mixing the reactants

Size of the prepared nanoparticles is depends on the rate at which the solution stir. Mechanism of Growth and nucleation both responsible for the size of nanoparticles. If growth rate is low as compared to the nucleation rate, Size of the prepared nanoparticles will be small and, If the growth rate is faster than the nucleation rate, Size of the prepared nanoparticles will be large [41].

3.8.3 Effect of pH

The size and shape of the prepared nanoparticle is also affected by pH of the solution. At low pH value there is no significant growth of nanoparticles. The growth rate of nanoparticles significantly increases at high pH value. When the value of pH is increased the time needed for synthesis is decreased. In case of nickel ferrite nanoparticles, the range of pH is 11-12.

3.8.4 Effect of temperature

In case of ferrite formation, different metals exhibit different activation energy values. The heat provided by reactants used in reaction gives rise to activation energy. The reaction temperature approximately ranges from 80°C to 100°C in case of the nickel ferrite nanoparticles in Co-precipitation reaction.

3.8.5 Heat treatment after Co-precipitation

Calcination is needed for single cubic phase formation after the completion of co-precipitation reaction. The shape and size of particles is also depend on amount of heat and the time for which the heat is applied. Impurities also removed during this heat treatment.

3.9 Synthesis of $Ni_{1-x}(CuAg)_xFe_2O_4$ Nanoparticles

Co-precipitation method is used for the synthesis of $Ni_{1-x}(CuAg)_xFe_2O_4$, where copper and silver used as dopant and x represent the dopant concentration which is x=0.0.025.0.05.

3.9.1 Chemical used:

Following are the chemical which are used during synthesis of $Ni_{1-x}(CuAg)_xFe_2O_4$ nanoparticles.

Table 3.1. Chemicals used in the synthesis process

Chemical names	Molecular formula	Molecular mass (g/mol)
Nickel Nitrate	$Ni(NO_3)_2.6H_2O$	290.80
Copper Nitrate	$Cu(NO_3)_2.3H_2O$	241.60
Silver Nitrate	$Ag(NO_3)_2.H_2O$	169.87
Iron Nitrate	$Fe(NO_3)_3.9H_2O$	404.00
Sodium Hydroxide	NaOH	40.00

Above mentioned materials are provided by ACROS Organics, EMSURE® Merck KGaA Darmstadt Germany and Fischer Chemical Ltd. – Hong Kong.

3.9.2 Apparatus used

Following are the apparatus used during the synthesis of $Ni_{1-x}(CuAg)_xFe_2O_4$ nanoparticles.

- Hot plates
- Magnetic stirrers
- Beakers
- Measuring balance
- Muffle furnace

- Ultra Sonicator

3.9.3 Co-precipitation route for the synthesis of $Ni_{1-x}(CuAg)_xFe_2O_4$ nanoparticles

For the preparation of undoped $NiFe_2O_4$ nanoparticles x=0. Calculated amount of nickel nitrate and iron nitrate were added into the 200ml of deionized water, solution was magnetically stirred for 10 to 20 minutes to obtain homogenous mixing. Deionized water was used to avoid impurities in final product. Mixture of nickel nitrate and iron nitrate were heated under the constant stirring upto 90^o C, On the other hand the solution of precipitating agent sodium hydroxide was already heated at 90^o C and mixed with the nitrated solution under constant stirring at the temperature of 90^o C. Then the solution was heated at 90^o C for the 45 mins under the constant stirring. After 45 minutes heating was turned off and pH of the solution was maintained at 12 at room temperature. Deionized water was used for washing the precipitates to obtain impurity free nickel ferrite nanoparticles. The water content was removed by drying the product in electric oven overnight at the temperature of 100^o C. The dried product was calcinated in muffle furnace for five hours at 800^o C. Similar procedure was followed for the doped nickel ferrites nanoparticles and the calculated amount of dopants was also added with nickel nitrate and iron nitrate into the deionized water and the remaining procedure was continued. Following is the stoichiometric formula used to calculate composition of different chemicals used in the process.

Mass = Molarity x Molecular Mass x 100/1000

Table 3.2. Synthesized Nanoparticles

Dopant Concentration (x) in $Ni_{1-x}(CuAg)_xFe_2O_4$	Prepared samples
0	$NiFe_2O_4$
0.25	$Ni_{0.75}(CuAg)_{0.25}Fe_2O_4$
0.5	$Ni_{0.5}(CuAg)_{0.5}Fe_2O_4$

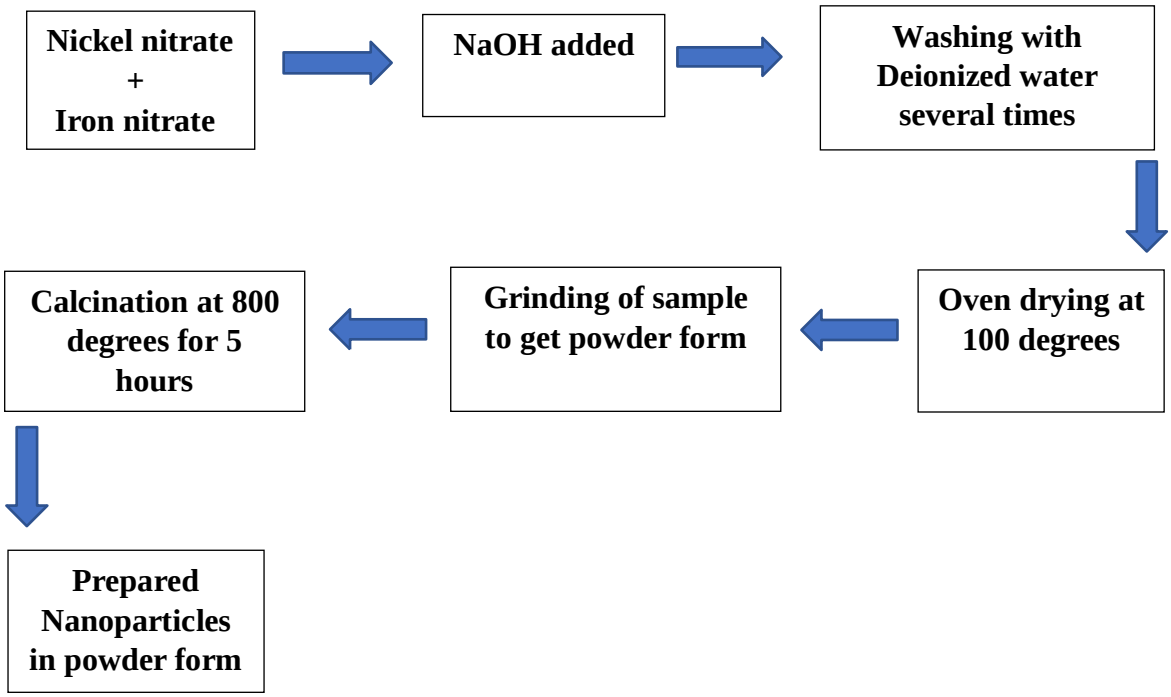

Figure 3.3. Synthesis route

3.10 Synthesis of $Ni_{0.05}(CuAg)_{0.05}Fe_2O_4$/Graphene platelets nanocomposites

Graphene platelets provided by Sigma Aldrich and already synthesized $Ni_{0.05}(CuAg)_{0.05}Fe_2O_4$ nanoparticles were used to prepare the nanocomposites by using ultrasonication method. 1.5 grams of $Ni_{0.05}(CuAg)_{0.05}Fe_2O_4$ nanoparticles were added into 50ml deionized water. Different percentage of graphene platelets (2% and 3.5%) were also added into the deionized water and the mixture was sonicated for 16 to 18 hours at room temperature, then the solution was dried over night at 100 ^{o}C. After drying, the agate mortar and pestle was used for the homogenized mixing of dried powder.

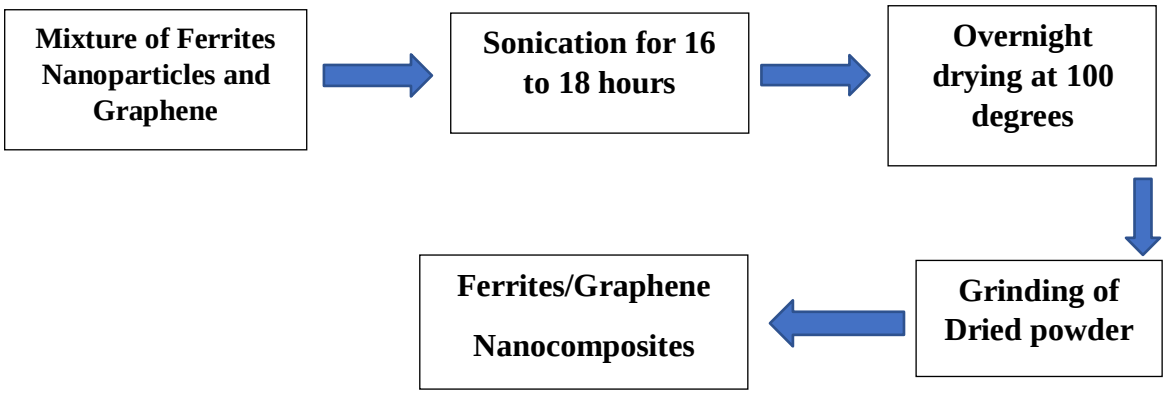

Figure 3.4. Synthesis of Nanocomposites

3.11 Water as a dispersive medium

The water is polar in nature. This polarity makes water a good solvent medium for ionic or polar solutes. Water molecules surround the ionic or polar molecule as it enters the water. This process is known as hydration. One solute molecule is surrounded by many water molecules as the size of water molecules is small. The partially negative end of water molecule is attracted towards partially positive end of solute molecule. This is known as hydrogen bonding. The sodium chloride salt is an example of ionic solute. It splits in to cations and anions and these ions are surrounded by water molecules. In this way these molecules are carried away from there crystal lattice in to solution. Sugar is an example of non-ionic solute. The dipole region of sugar molecules makes hydrogen bonding with water dipoles. In this way sugar is mixed in to solution.

Table 3.3. Synthesized Nanocomposites

Graphene (wt.%)	Prepared Nano composites
2 %	$Ni_{0.75}(CuAg)_{0.5}Fe_2O_4$ + 2%
3.5%	$Ni_{0.75}(CuAg)_{0.5}Fe_2O_4$+ 3.5%

Chapter 4

Characterization Techniques

The properties of synthesized nickel ferrite nanoparticles with graphene loadings are analyzed by performing some specific analysis techniques. Properties like physical and chemical properties and other information about material such as morphology, lattice parameter, structure etc. can be obtained using one of the analysis techniques. This chapter will cover a short introduction of the characterization techniques. Following characterization techniques can be used for the analysis of synthesized composite.

4.1 X-Ray diffraction technique

It is a useful tool for the identification of degree of crystallinity and structure of a material. Clear information about structural strain, crystal defects, average crystallite size, crystallographic orientation and degree of crystallinity can be obtained using XRD [42]. Three different methods can be used for finding out crystal structure i.e. powder diffraction method, Laue method and rotating crystal method. Two techniques can be used to determine crystal size if powder diffraction method is used. Those techniques are as follows.

- Debye Sherrer Method
- Diffractometer method

The sample was in the form of fine grinded powder. Copper, Molybdenum etc. can be used as a target material. Cu-kalpha=1.54 Å source was the XRD source used for analysis in this case.

4.1.1 Basic principle of XRD

The powdered sample is placed for analysis. X-ray beam is made to fall on the sample and reflected from plane of crystal. The crystal plane reflects the X-rays that are incident on material. The interference only takes place when incidence angle is exactly same as reflection angle. The Bragg's Law is given by

$$n\lambda = 2d\sin\theta \quad \text{.....(4.1)}$$

n is order of interference, θ is incidence angle, d is Interlayer distance and λ is incident X-ray wavelength. The Bragg's law states that the incident ray is reflected only when the path difference between set of planes is 2dsinθ [43]**.** The set of planes are at an equal distance of d. Following is the condition required for constructive interference:

$$2d\sin\theta = n\lambda, \text{ where } n=1,2,3\ldots..$$

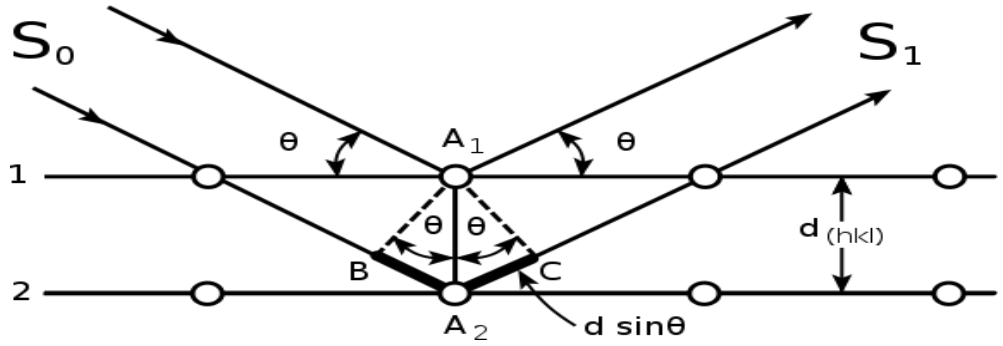

Figure 4. 1.Incident x-ray beam scattered by atomic plane in a crystal [44]

The equation is known as Bragg's equation. The condition for reflection in above mentioned equation is that it only occur when θ<2d. For this reason visible light cannot be used. For the characterization of a three dimensional structure three techniques are usually used which are as follows:

- Laue Method
- Powder method

- Rotating Crystal Method

The sample which is to be characterized using XRD is in the form of Nano powder. So the powder method will be the one useful for the desired sample. For the evaluation of powdered sample and in the case of in availability of single crystal of acceptable size, powder diffraction is the best method to be employed. The procedure of this experiment includes the crushing of sample in to fine powder. Afterwards the sample will be placed in aluminium or glass rectangular shaped plate. A monochromatic X-ray beam is then directed towards the powdered sample.

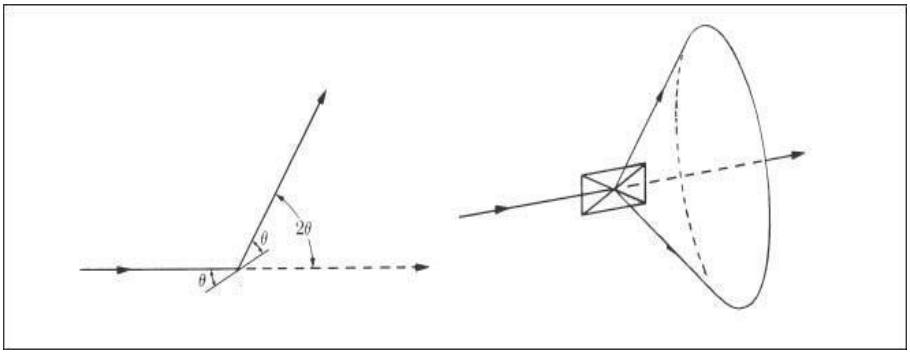

Figure 4. 2.X-ray Diffraction [44]

Consider the reflection as shown in figure. The fraction of sample, which is in powder form, is at such an orientation which will enable reflection by being present at correct Bragg angles. When the plane is rotated about the beam which is made incident, the path of motion of reflected beam will be across the surface of cone. In the case of our particles the reflection does not occur across the surface, a large number of crystal particles will have same reflections and some of those reflections will be able to satisfy brags law. The inter plannerspacing, d, can be calculated by knowing values of λ and θ.

- **Lattice constant**

Lattice constant defines the unit cell of a crystal. It is the length of one edge of the cell or an angle forming between edges. It can also be termed as lattice constant or lattice parameter. The

distance, which is constant, between the lattice points is known as lattice constant. Following equation is used to calculate lattice constant.

$$a=d_{hkl}\ (h^2+k^2+l^2)^{1/2} \quad \text{.....(4.2)}$$

In the above equation, lattice constant is "a", the wavelength of X-ray radiation is 1.54 for Cukα, miller indices are "*h, k, l*" and diffraction angle is θ.

- **Crystallite size**

For the identification and confirmation of the experimentally obtained diffraction pattern it is compared to JCPDS cards. The structural properties are greatly influenced by particle size. According to Debay Sherrer equation, which is used to calculate particle size, crystal size is inversely proportional to peak width. So the small crystallite size is related to peak broadening in XRD analysis. The Debay sherrer equation is used to calculate particle size.

$$t=\frac{0.9\ \lambda}{\beta\ cos\theta} \quad \text{..... .....(4.3)}$$

λ represents the incident X-ray wavelength and θ and β represent diffraction angle and full width half maximum respectively.

- **X-Ray density**

The X-ray diffraction data can be used for the calculation of sample material's density [45]. If the lattice constant is known for each sample following formula will be used.

$$\rho_x = \frac{8M}{Na3} \quad \text{.....(4.4)}$$

Where ε represents molecular weight of sample, N is the Avogadro's number ($6.03x10^{23}$) and "a" is the lattice constant. Eight formula units are possessed by each cell.

- **Measured density**

The intrinsic properties of materials define the bulk density or measured density. The density formula is generally used for the density calculation.

$$\rho_m = \frac{m}{\pi r 2h} \quad \text{..... (4.5)}$$

Where m represents the mass, r represents the radius; h is the thickness of the pressed pellet sample.

For the calculation of measured density, a circular pallet is made using hydraulic press which compact the powdered sample. Vernier caliper is used for measuring thickness and radius of pallet and analytical balance is used for measuring mass of the pallet. The measured parameters are substituted in equation for the resultant density calculation.

- **Porosity fraction**

Along with the alternation in compositions, the increase in the porosity fraction is observed. Following formula is used for calculation of porosity fraction.

$$\text{Porosity Fraction} = \frac{I - \rho m}{\overline{\rho x}} \quad \text{..... (4.6)}$$

4.2. Scanning electron microscopy

Scanning electron microscopy is an imaging technique which makes use of high energy electron beams for imaging Nano and bulk surfaces. When the highly energetic beam strikes the sample surface it provides following information.

- Composition of the sample.
- Phase mapping
- Topography of the sample.

When the beam hits the surface of material there will be various kind of interactions and signals are emitted as a result of these interactions such as transmitted electrons, back scattered electrons, secondary electrons, cathode luminiscence and characteristic X-rays [46].

4.2.1 Basic principle of SEM

The beam of electron is made to focus on the surface of sample in scanning electron microscopy. The raster scan is used which can focus on very narrow cross sectional area. The surface of sample will emit electrons or photons when the incident electron beam interacts with the surface. Different sets of detectors are employed to collect the emitted photons and electrons. The brightness of the cathode ray tube is controlled by using the outputs of detectors. The X and Y input of cathode ray tube are adjusted in relation with X and Y voltages rastering the beam of electron. As a result image is obtained on cathode ray tube display. Images are produced by backscattered electrons, elemental x-rays and secondary electrons.

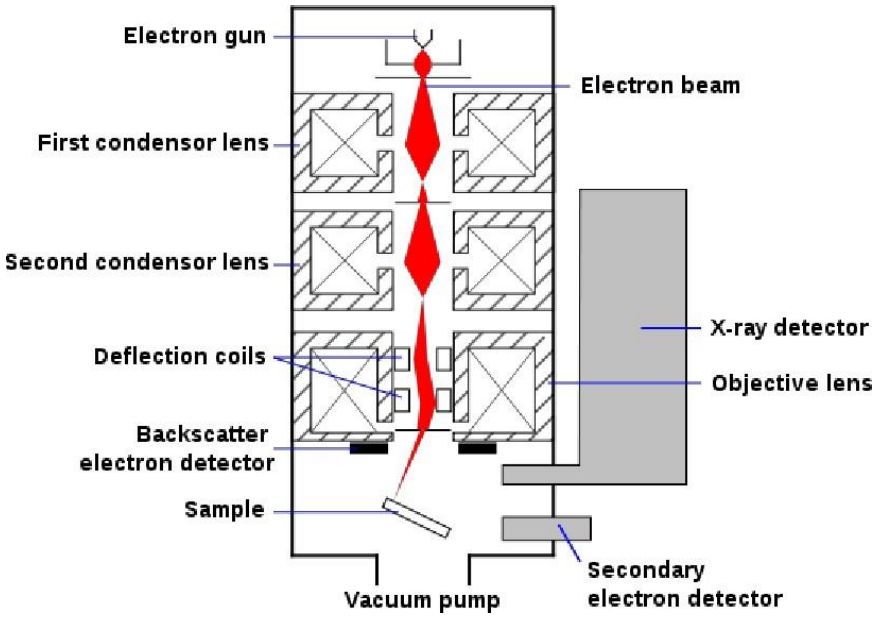

Figure 4. 3. Schematic figure of scanning electron microscope [47]

4.3. Fourier transform infrared spectroscopy

The absorption, emission spectra's, Raman scattering and photoconductivity of the material can be obtained by using this analytical technique. The stretching modes of the elements present in composite and chemical purity of the sample can be determined using FTIR. It is known as FTIR because it involves the Fourier, a mathematical term. It collects the data from spectrum of matter. FTIR is used to determine the amount of light that a sample absorbs at a specific wavelength.

4.3.1 Working of FTIR

In FTIR, an infrared light beam from a source which is polychromatic is made to fall on splitters. Half portion of the incident light is refracted towards fixed mirror and other half of the incident light is transmitted through a moving mirror. Transmitted light pass through the sample. The information about molecular component and structure of the sample can be obtained by interaction of light with sample.

4.3.2 Applications of FTIR

A gas chromatograph is used to separate the components of a mixture

- The analysis of liquid chromatography fraction can be done using FTIR.
- Tiny samples can be checked with the help of infrared microscope in sample chamber.
- The sample acquiring emitted spectrum of light is obtained FTIR instead of light spectrum through the sample [24]

4.4. Electrical Properties

4.4.1 Dielectric properties

The LCR meter bridge is used for determination of dielectric properties such as dielectric loss, dielectric constant etc. Firstly the capacitance of pallets were find out using LCR meter then following formula is used for the calculations of dielectric constant.

$$\epsilon' = \frac{Cd}{A\epsilon o} \quad \text{……..……(4.7)}$$

Where C represents the capacitance of the pellet (farad), t represents the thickness of the pellet (Meters), A represents the cross-sectional area of the flat surface of the pellet and 0 is the constant of permittivity for free space and its value is equal to 8.85x10-12 F/m. The imaginary part that corresponds to the energy dissipation losses is calculated by using the following equation:

ε"= ε*D….....(4.8)

There are different types of polarization which take place in dielectric materials when the

Interact with the applied field.

4.4.2 Electronic and Atomic polarization

When the dielectric material is placed within the electric field the electron cloud of atoms is displaced relative to nuclei in atom, which produce an induced dipole moment in the molecule.

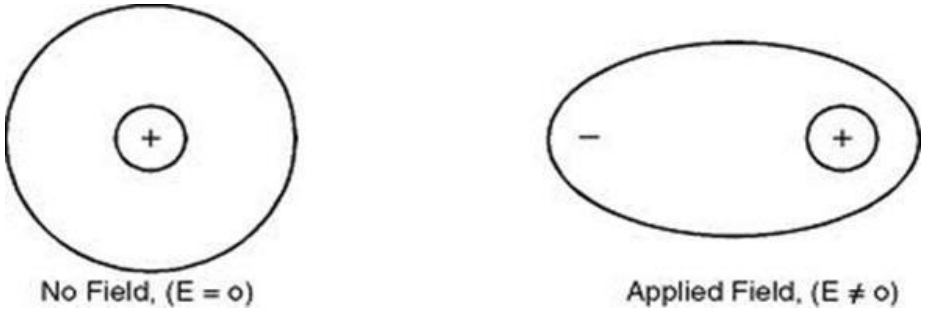

Figure 4. 4. Electronic polarization[45]

4.4.3 Ionic Polarization

Ionic polarization take place in solids with ionic bonding having dipoles, but these dipoles get cancel due to the symmetry of the crystals structure. In the presence of applied electric field positive and negative ions are displaced from their equilibrium positions hence inducing dipole moment.

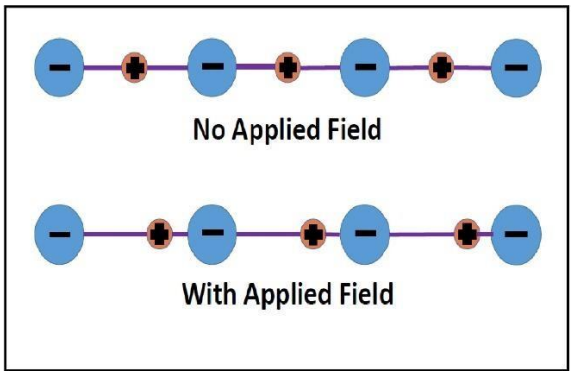

Figure 4. 5. Ionic polarization[45]

4.4.4 Dipolar and Orientation Polarization

It is only applicable to the polar dielectric materials. In the absence of electric field dipoles are randomly oriented so the sum of their dipole moment is zero. When these polar dielectric materials are placed within the electric field these dipoles rotate and align themselves in the direction of electric field.

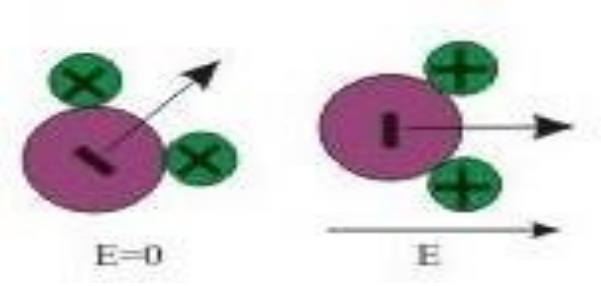

Figure 4.6. Dipolar polarization[45]

4.4.5 Interface and space charge Polarization

Space charge polarization take place due to the diffusion of ions along with applied electric filed. It usually occurs due to the accumulation of charges in the interface or at the grain boundaries of the material

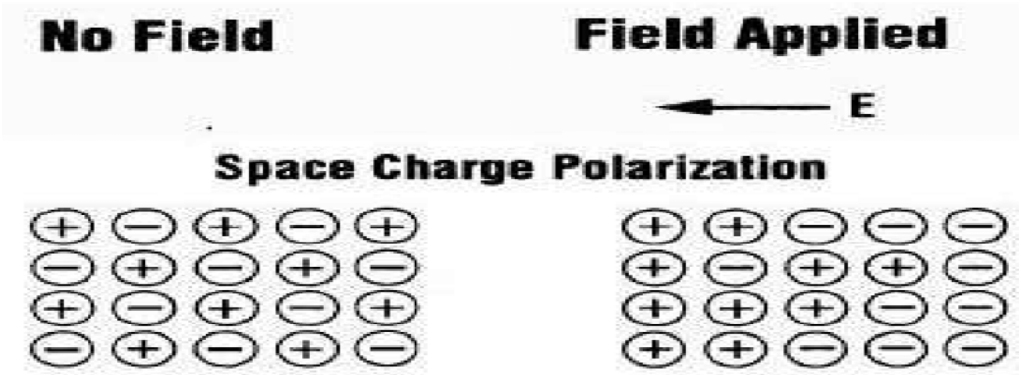

Figure 4.7. Space Charge polarization[45]

Results and Discussion

5.1. X-ray Diffraction

The knowledge of phase formation and exploration of structure was obtained using XRD technique. The prepared sample was finely grounded and annealed before subjecting it to XRD machine.

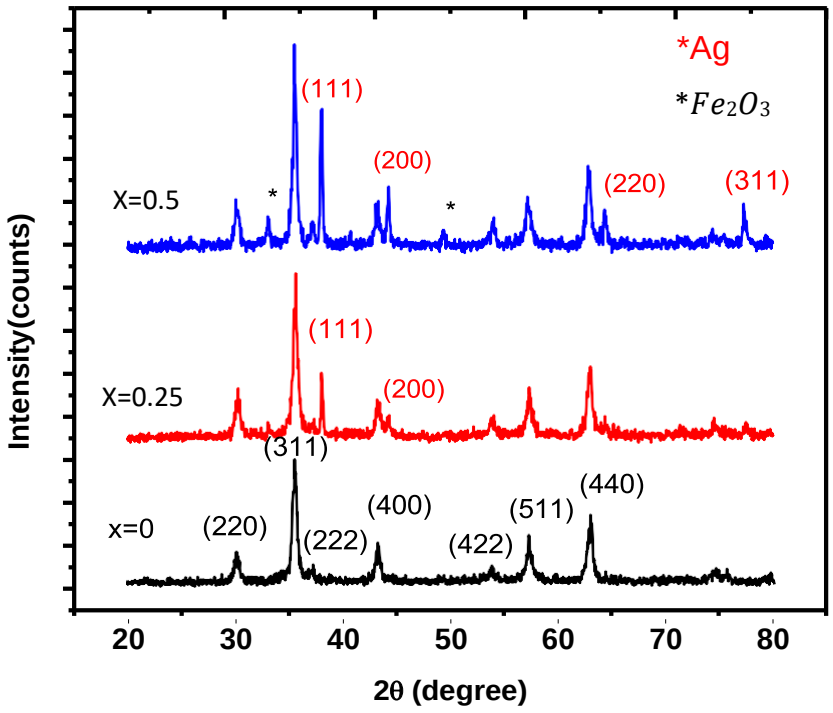

Figure 5. 1. XRD pattern of copper silver doped Nickel Ferrites Nanoparticles

The above mention figure shows the XRD pattern of $Ni_{1-x}(CuAg)_xFe_2O_4$,where x=0, 0.25 ,0.5. It shows all the characteristics peaks. The peaks were indexed by comparing with the JCPDS card # 01-087-2335 (220), (311),(222),(400), (422),(511) and (440) [47]. XRD pattern

reveals that nickel ferrite nanoparticles exhibit single phase spinel cubic structure. As copper and silver were introduced in nickel ferrites as a dopant, separate peaks due to the addition of silver were formed. There was no separate peak due to the addition of copper because of the small difference between the ionic radii of copper and nickel [15]. The ionic radii of $Ni^{2+}$is (0.69Å) and $Cu^{2+}$is (0.73 Å). so, as the ionic radii of copper and nickel were comparable , Cu^{2+} simply replaced the Ni^{2+} present on the octahedral sites. It was observed that as the concentration of dopants increases up to x=0.5 secondary hematite phase started appearing (Fe_2O_3) this was due to the segregation of metallic silver ion on the grain boundaries as there was a significant difference between the ionic radii of Ag^{2+} (1.15 Å) and Ni^{2+}(0.69 Å).

The lattice parameters of the prepared nanoparticles were calculated using the following relation.

$$\mathbf{a= } \boldsymbol{d_{hkl}} \ (\boldsymbol{h^2 + k^2 + l^2})^{\mathbf{1/2}}$$

where 'a' represent the lattice parameter, hkl represent the miller indices of high intensity peak of prepared nanoparticles and d represent the D- spacing of that high intensity peak.

When both dopants were introduced into the crystal structure, the decrease in lattice parameter was observed, due to the significant difference in the ionic radii of Ag^{2+} (1.15 Å) and Ni^{2+}(0.69 Å). As Ag^{2+} ion could not enter completely into the crystal structure and exerted a pressure on the grain boundaries which lead to the decrease in lattice parameter, where Cu^{2+} (0.74 Å) and Ni^{2+}(0.69 Å) have comparable size so copper was incorporated into the system. As the amount of dopants reaches up to x=0.5 lattice parameter starts increasing due to the fact that copper and silver both have larger ionic radii as compared to nickel so as their concentration increases more Cu^{2+} ions replaced Ni^{2+} ion and few Ag^{2+} ion entered into system. When small ionic radii ion is replace by the large ionic radii ion lattice parameter increases.

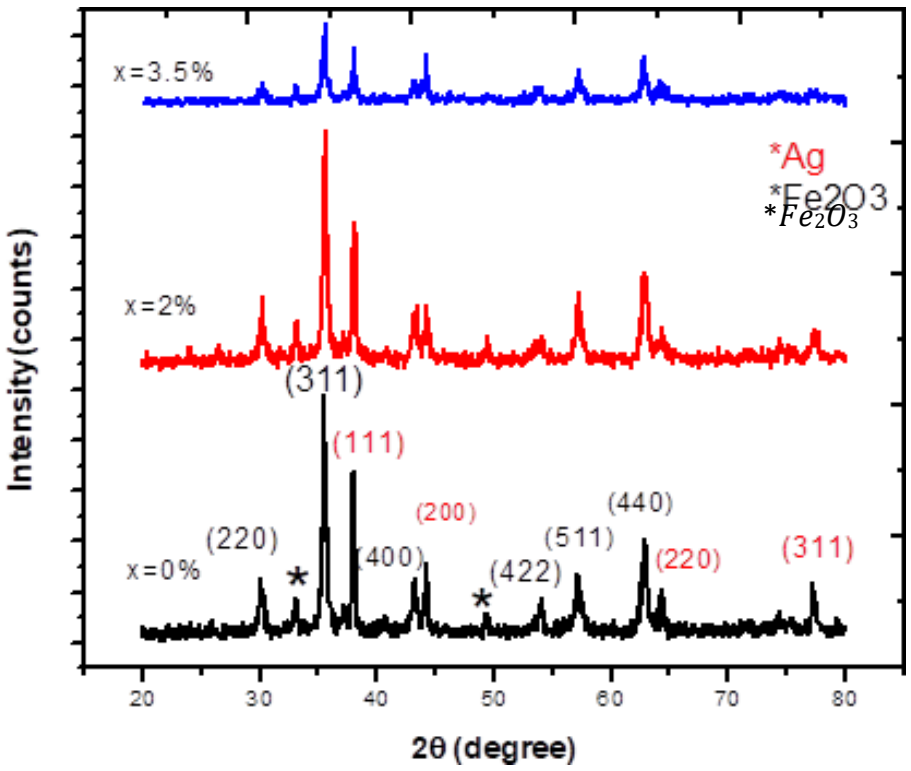

Figure 5.2 XRD pattern of Nanocomposites

The figure shows the XRD pattern of ferrites composites $Ni_{0.5}(CuAg)_{0.5}Fe_2O_4$ @Graphene where x= 0%, 2% and 3.5 %. The XRD pattern shows that there is no structural change in ferrites nanocomposites. The characteristics peak of graphene usually appears at 2θ = 26°As the concentration of graphene is very small relative to ferrites nanoparticles so characteristics peak does not appear, it usually appear when the graphene concentration exceed from 10%. However, intensities of the ferrites peaks decrease as the graphene concentration increases which indicated that graphene sheets cover the ferrites nanoparticles.

Table.5. 1. Variation in X-ray density, bulk density, porosity, lattice parameter and crystallite size in prepared ferrites nanoparticles and nanocomposites

Prepared Samples	X-ray-density g/cm^3	Bulk density g/cm^3	Porosity (%)	Lattice parameter (Å)	Crystallite size (nm)
$NiFe_2O_4$	5.29	2.66	50	8.37	17.66
$Ni_{0.75}(CuAg)_{0.25}Fe_2O_4$	5.36	2.75	49	8.36	21.19
$Ni_{0.5}(CuAg)_{0.5}Fe_2O_4$	5.38	3.33	37	8.38	53.00
$Ni_{0.5}(CuAg)_{0.5}Fe_2O_4$+ 2%G	5.39	2.85	47	8.38	53.00
$Ni_{0.5}(CuAg)_{0.5}Fe_2O_4$+ 3.5%G	5.40	2.75	50	8.38	53.00

It was observed from the above-mentioned table that X-ray density increases as the concentration of dopant increases due to the increase in molecular weight, similar trend is observed for Ferrites and Graphene nanocomposites. Trend of bulk density is different from the X-ray density, It was observed that as the copper and silver were added into the nickel ferrites system due to their larger ionic radii than nickel pores and void spaces in the structure is decreases so the bulk density increases and porosity decreases as the bulk density is inversely related to the porosity.In case of $Ni_{0.5}(CuAg)_{0.5}Fe_2O_4$@Graphene nanocomposites opposite trend of bulk density was observed that the bulk density start decreases in the nanocomposites due to the porous nature of the graphene and porosity increases for the ferrites and graphene nanocomposites.

5.2 Fourier transform infrared spectroscopy.

For FTIR analysis, In KBr pellets, powdered samples of nickel ferrites and doped nickel nanoparticles, and their composites with graphene were incorporated. Then, their spectra were obtained within range of 4000 cm^{-1} to 350 cm^{-1} using FTIR spectrophotometer (FTIR PerkinElmer-spectrum 100)

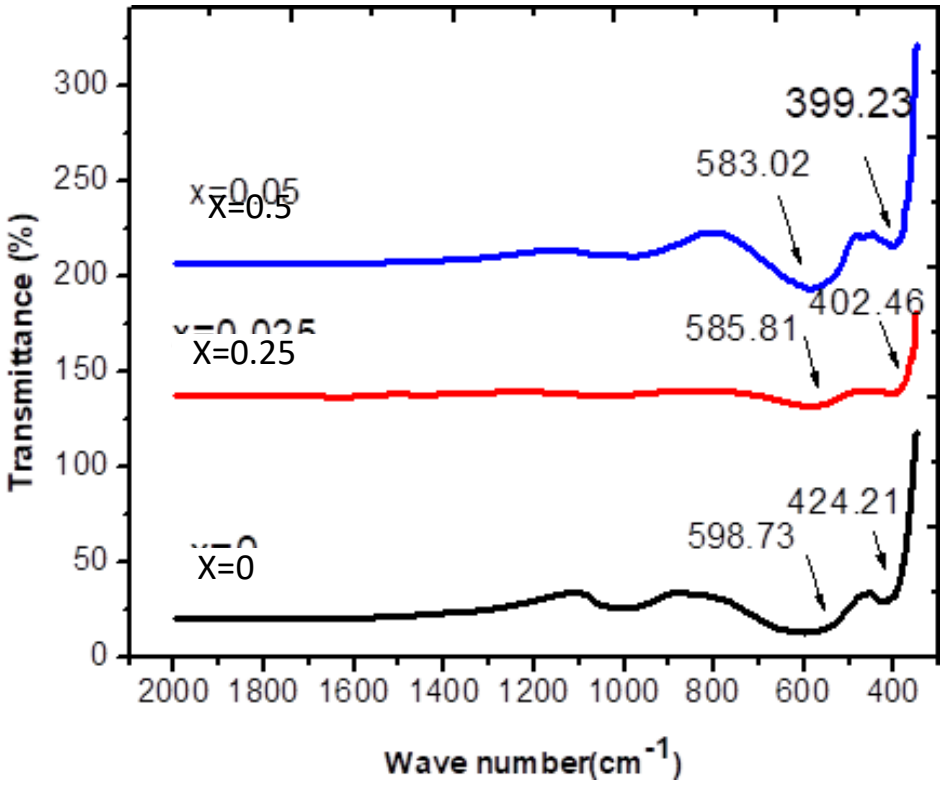

Figure 5. 3 FTIR of copper silver doped Nickel Ferrites Nanoparticles

Fig 5.3 shows the FTIR spectra of synthesized nanoparticles of $Ni_{1-x}(CuAg)_xFe_2O_4$. The two characteristics bands of spinel ferrites observed in FTIR pattern. The band at v_1 ranges from (399 cm^{-1} to 430 cm^{-1}) represents the octahedral site of the spinel ferrites and the band at v_2 ranges from (580 cm^{-1} to 600 cm^{-1}) represents the tetrahedral site of the spinel ferrites. The band v_1 is assigned to the intrinsic vibration of the octahedral site where metal ion-oxygen bonds are presents. The band v_2 is assigned to the intrinsic stretching vibrations of the tetrahedral sites. The presence of theses absorption bands in FTIR spectra confirms the

synthesis of the single phase cubic spinel structure [16]. It was observed as the copper and silver were doped into the system and their concentration increases both v_1 and v_2 shifts towards the lower frequency side which may due to the distribution of cations into the spinel lattice. Silver and copper enter the tetrahedral sites having larger ionic radii which results in partial migration of Fe^{3+} ions from tetrahedral to octahedral site, which contributes to the larger bond length in tetrahedral site. Since the vibration frequency is proportional to the force constant so with the increases in dopants concentration the force constant decreases. Following relation is used to calculate the force constant

$$F = 4\pi^2 c^2 v^2 \mu$$

Where F is the force constant, c is the velocity of light $2.99*10^8$ m/s, υ is the vibration frequency of tetrahedral and octahedral sites, u is the reduced mass for the Fe^{3+} ions and the O^{2-} ions ($2.065*10^{-23}$g) [16].

Table.5. 2. FTIR transmittance bands of Nanoparticles

Samples	Octahedral band υ_1 (cm^{-1})	Tetrahedral band υ_2 (cm^{-1})	Force constant F_{Oct}(dyne/cm^2)	Force constant F_{tet}(dyne/cm^2)
$NiFe_2O_4$	424.21	598.73	$1.31*10^5$	$2.62*10^5$
$Ni_{0.75}(CuAg)_{0.25}Fe_2O_4$	402.46	585.81	$1.18*10^5$	$2.51*10^5$
$Ni_{0.5}(CuAg)_{0.5}Fe_2O_4$	399.23	583.02	$1.16*10^5$	$2.49*10^5$

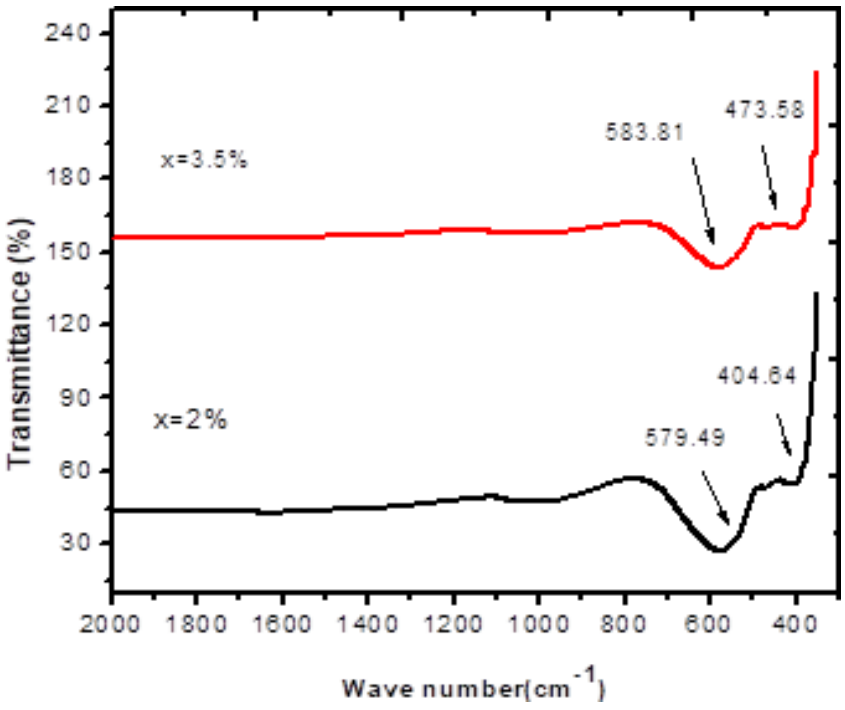

Figure 5. 4 FTIR of Nano composites

Figure 5.4 shows the FTIR of $Ni_{0.05}(CuAg)_{0.05}Fe_2O_4$@Graphene, where x= 2% and 3.5%.The characteristics bands shows the tetrahedral and octahedral sites of Ferrites, But for the composites we have additional extras peaks at 1621-1680 cm-1 and 3406-3500 attributes to the C=C and O-H deformation bands respectively [48].

Table.5. 3 FTIR transmittance bands of Nanocomposites

Samples	**Graphene** (wt.%)	**Octahedral band** υ_1 (cm^{-1})	**Tetrahedral band** υ_2 (cm^{-1})	**Force constant** F_{Oct}(dyne/cm^2)	**Force constant** F_{tet}(dyne/cm^2)
$Ni_{0.5}(CuAg)_{0.5}Fe_2O_4$	2%	404.64	579.49	$1.19*10^5$	$2.46*10^5$
$Ni_{0.5}(CuAg)_{0.5}Fe_2O_4$	3.5%	473.58	583.81	$1.64*10^5$	$2.49*10^5$

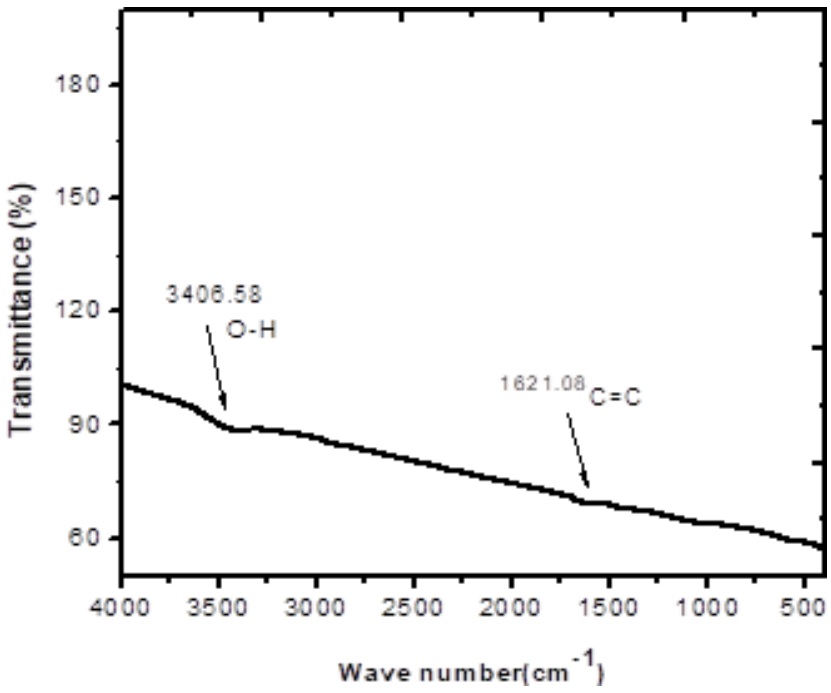

Figure 5. 5 FTIR of Graphene

5.3 Scanning Electron Microscopy Results

SEM images of $Ni_{1-x}(CuAg)_xFe_2O_4$, shown in the figure 5.6 at different magnification. SEM images reveals that synthesized nanoparticles are uniformly and well dispersed and no agglomeration was observed. Prepared nanoparticle's size distribution lie in the range of 17 to 25 nm. It can be observed that particles are fine, having spherical morphology with no agglomeration.

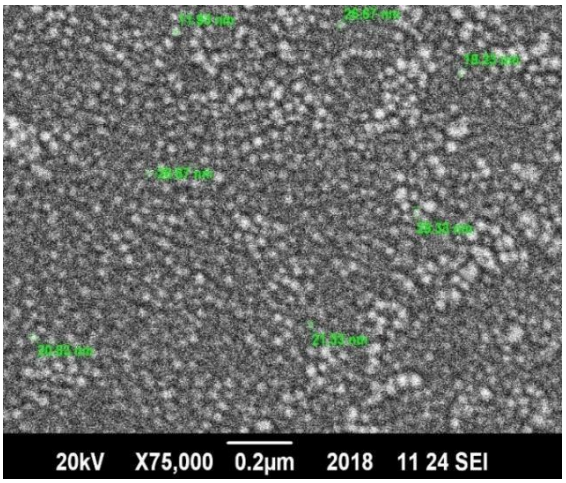

Figure 5. 6 SEM images of Nickel Ferrites Nanoparticles

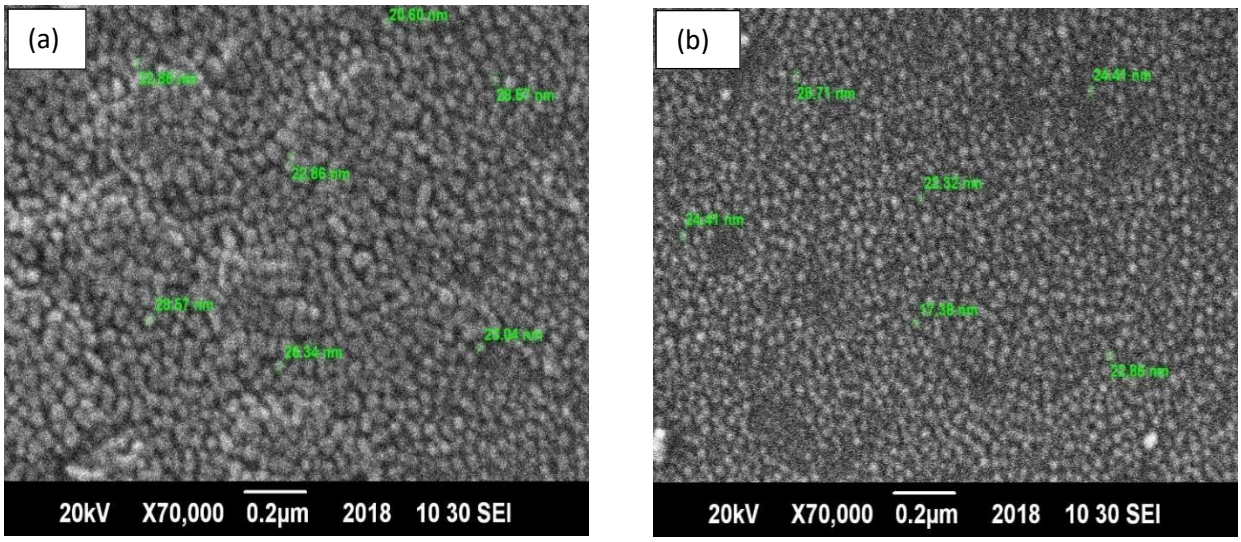

Figure 5.7 SEM images of Doped Nickel Ferrites Nanoparticles

Figure 5.7 (**a**) show the SEM images of $Ni_{0.75}(CuAg)_{0.25}Fe_2O_4$ and Figure 5.7 (**b**) show the SEM image of $Ni_{0.5}(CuAg)_{0.5}Fe_2O_4$**.**

5.3.1 SEM Images of $Ni_{0.5}(CuAg)_{0.5}Fe_2O_4$@ Graphene:

Following are the SEM images of $Ni_{0.5}(CuAg)_{0.5}Fe_2O_4$@ Graphene nanocomposites with 2% and 3.5% graphene. SEM images of Nanocomposites reveal that ferrites nanoparticles are uniformly decorated along the surface of graphene sheet without any noticeable agglomeration.

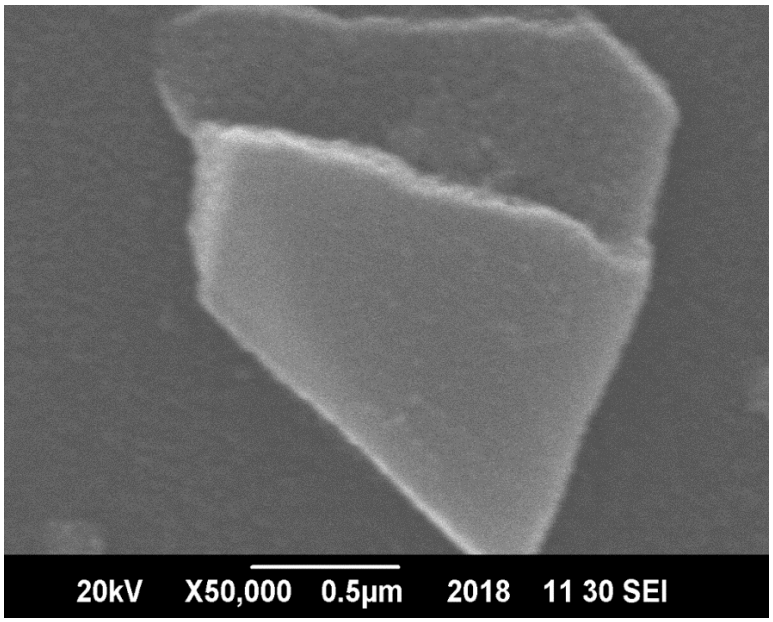

Figure 5. 8 SEM image of Pure Graphene

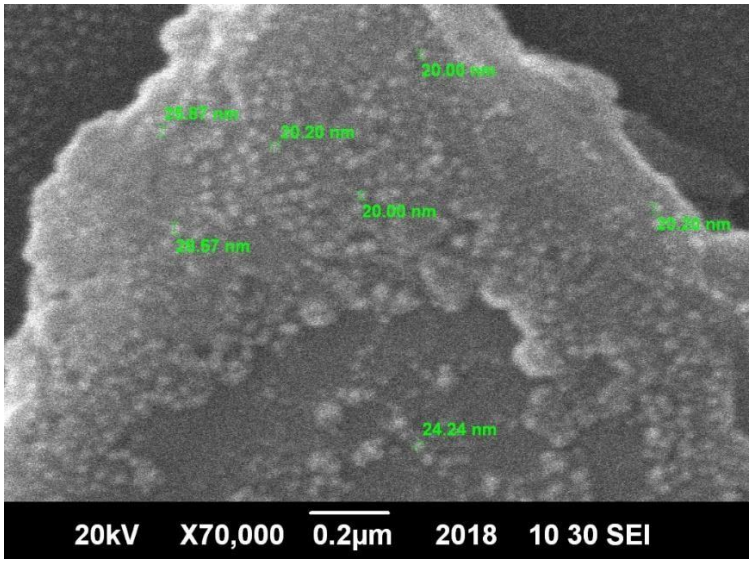

Figure 5. 9 SEM image of Ferrites with 2% Graphene

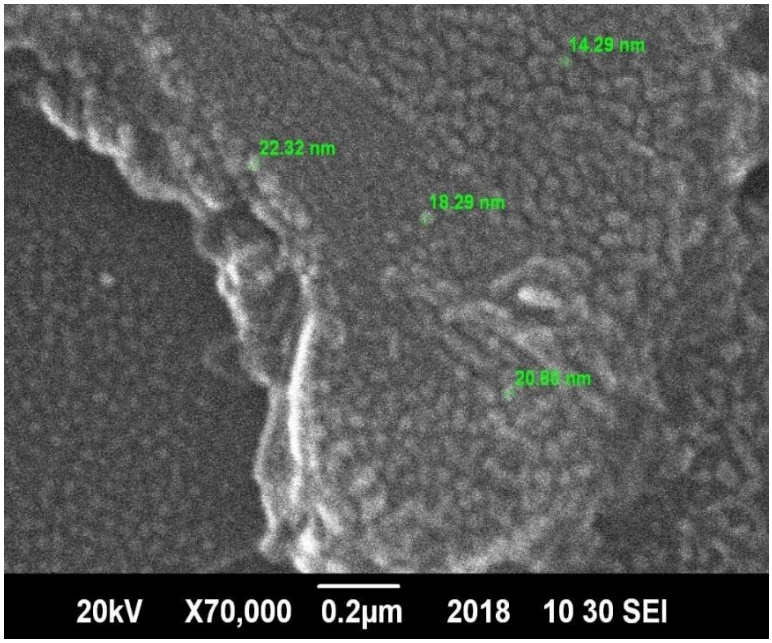

Figure 5. 10 SEM image of Ferrites with 3.5% Graphene

5.4. Dielectric studies

Wayne Kerr Precision Impedance analyser was used to investigate the dependence of Dielectric properties such as dielectric constant, Dielectric loss, tangent loss, Ac conductivity, impedance with respect to Frequency. Pallets were prepared and sintered for the calculations. Dielectric materials are considered as an electric insulator, but they have the ability to polarize their dipoles in the presence of applied electric field. The study of dielectric properties is related to the storage and dissipation of electrical and magnetic field and these properties are important for describing various mechanism in the fields of electronic, optics and solid-state physics.

5.5 Dielectric Constant

Dielectric constant of the material also known as the permittivity of the material represents the ability of a material to store electrical energy under the influence of electric field. Dielectric constant exhibit real and imaginary part. Its real part deal with the ability of a material to undergo a process of polarization in the presence of applied electric field. Figure 5.14 shows the trend of dielectric constant in $Ni_{1-x}(CuAg)_xFe_2O_4$.

Dielectric constant measure across the frequency range of 1MHz to 1GHz. It was observed that as the frequency increases dielectric constant of each sample is decrease. This trend shows the normal behaviour of cubic ferrites. Max-well and Wagner explain the dielectric behaviour with respect to frequency [49].They proposed the two-layer model and according to that model, dielectric materials having inhomogeneous structure exhibits conducting grains which are separated by insulating grains. When the dielectric constant is placed under the electric field, the electrons arrive at the grain boundaries through the mechanism of hopping. Due to the resistive nature of the grain boundaries electrons add up here and produce space charge polarization. These charge carriers take some time to align along the applied electric field. So when the frequency increases only few electrons are able to reach the grain boundaries and charges do not line up with the applied field as a result polarization decreases and dielectric constant also decreases with the increase in frequency [15]. Now as the copper and silver enter into the nickel ferrites nanoparticles, it was observed that dielectric constant increases as compared to the undoped nickel ferrites nanoparticles, the reason behind this is that Cu^{2+} and Ag^{2+}ions replace the few Ni^{2+} ion from octahedral sites and some Fe^{3+} ions from the tetrahedral sites as a result Fe^{3+} ions migrate from tetrahedral sites to the octahedral sites, and on the octahedral site concentration of Fe^{3+} and Fe^{2+} charge carriers increases which lead to the increase in hopping mechanism of electrons between Fe^{3+} and Fe^{2+}, Consequently polarization and dielectric constant increases [50].

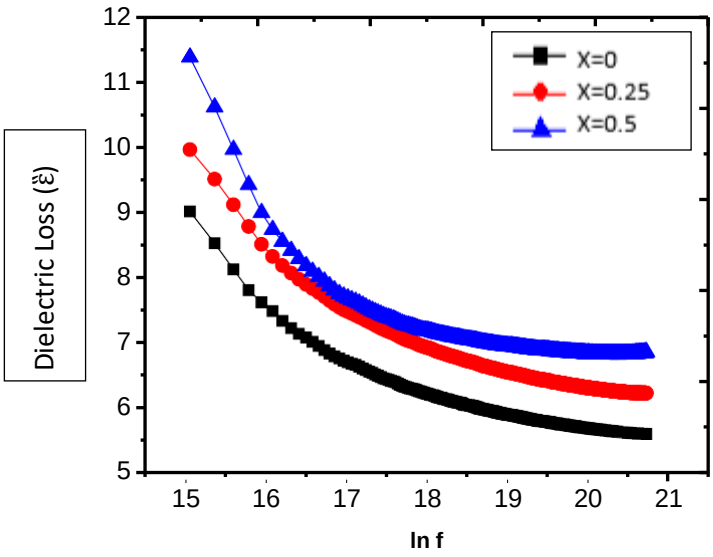

Figure 5. 11 Dielectric constant of copper silver doped Nickel Ferrites Nanoparticles

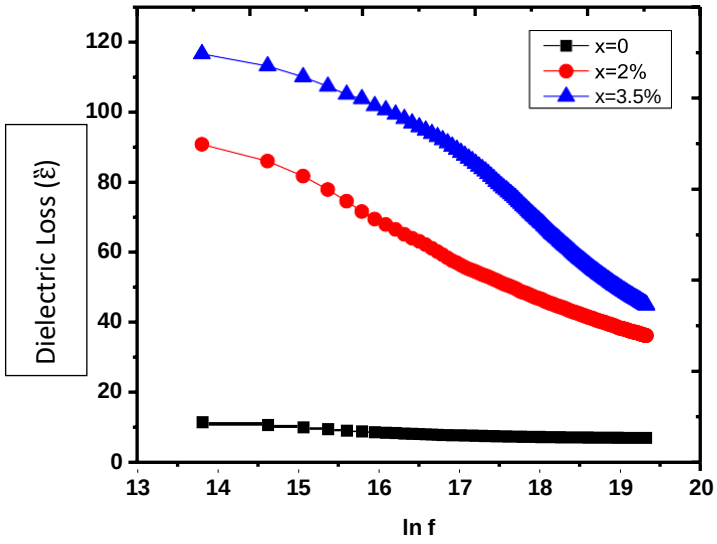

Figure 5. 12 Dielectric Constant of Ferrites and Graphene Nanocomposites

Figure 5.15 shows the Dielectric constant of $Ni_{0.5}(CuAg)_{0.5}Fe_2O_4$ @Graphene where x= 2% and 3.5%.It was observed that dielectric constant of ferrites further increases as the percentage of graphene increases in the Nano composites, this is due to the conductive network of graphene which enhances the dielectric constant of ferrites. Graphene is an allotropic form of carbon where carbon atoms are tightly bound to form ha hexagonal lattice structure. The high mobility pi electrons are located above and below the graphene sheet. Excellent electronic conductivity of graphene is dictated by the bonding and antibonding of these pi electrons.

5.6 Dielectric loss

Dielectric loss is the imaginary part and it is associated to the amount of energy dissipated. Figure 5.16 shows the variation of dielectric loss with the frequency. Dielectric loss also decreases with the increase in frequency. As the copper and silver are doped into the nickel ferrites nanoparticles dielectric loss increases as compared to the undoped nickel ferrites nanoparticles. Koop's theory explains the behaviour of dielectric loss in terms of the grain boundaries. According to the theory at low frequency grain boundaries become active and extra

resistive, as a result mechanism of polarization require more energy and this will cause the high values of dielectric loss [51].

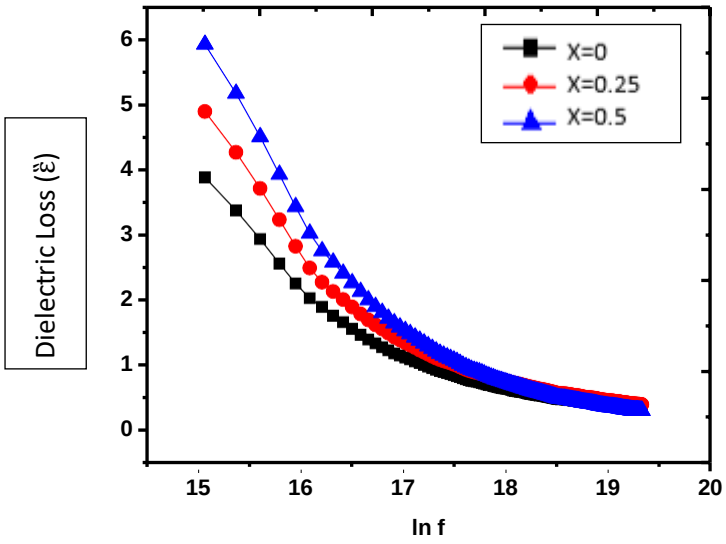

Figure 5. 13 Dielectric loss of copper silver doped nickel ferrites nanoparticles

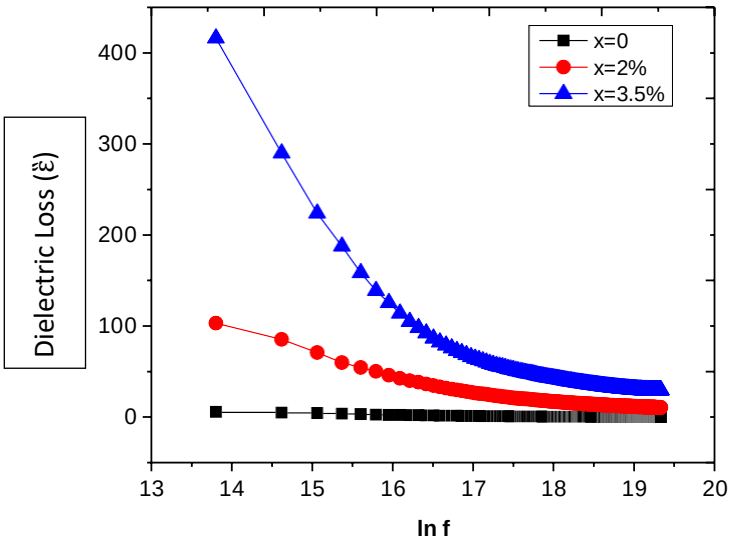

Figure 5.14 Dielectric loss of ferrites and graphene nanocomposites

Figure 5.17 shows the Dielectric loss of $Ni_{0.5}(CuAeg)_{0.5}Fe_2O_4$ @Graphene where x= 2% and 3.5 %. It was observed that dielectric loss is further enhanced with the addition of graphene due to the large surface area of graphene which increases the number of voids and interfaces present between the graphene and ferrites nanoparticles.

5.7. Dielectric Tangent Loss

The Dielectric tangent loss is studied at room temperature as a function of frequency. Figure 5.18 shows that dielectric tangent loss decreases as the frequency increases. Dielectric tangent loss is the ratio of dielectric loss to the dielectric constant. The value of tangent loss depends on various factors like stoichiometry, structure homogeneity. As the concentration of dopants increases dielectric tangent loss also increases because the grain boundaries are more active and provide resistance to the charge carriers, so more energy is required for the mechanism of polarization.

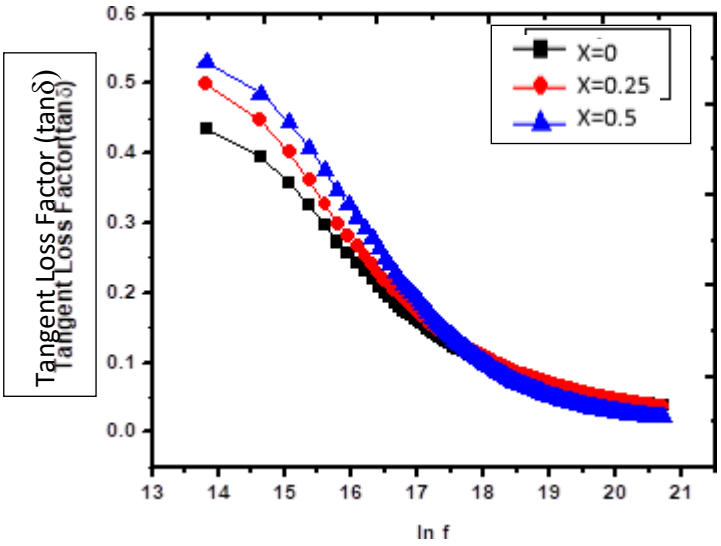

Figure 5. 15 Dielectric tangent loss of copper silver doped nickel ferrites nanoparticles

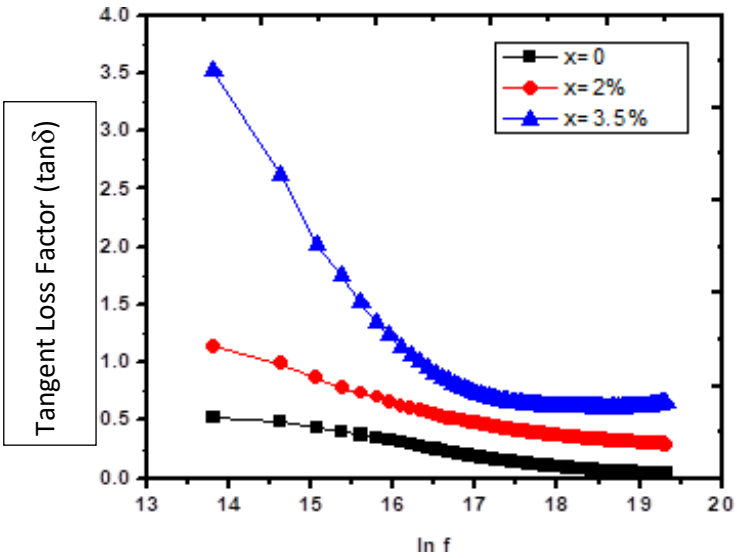

Figure 5. 16.Dielectric tangent loss of ferrites and graphene nanocomposites

Figure 5.19 shows the Dielectric tangent loss of $Ni_{0.5}(CuAg)_{0.5}Fe_2O_4$ @Graphene where x= 2% and 3.5 %. With the addition of graphene dielectric tangent loss further increases due to the conductive nature and large surface area of graphene. The pi electrons of graphene contributes

toward the conduction mechanism and its help in electron hopping between same type of ions.

5.8. AC Conductivity

The AC conductivity in the frequency range of 1MHz to 1GHz was calculated from the data of dielectric studies using the following relation.

$$\sigma_{a\,c} = \omega\, \varepsilon_o\, \varepsilon' \,\mathrm{Tan}\, \delta$$

Where $\omega=2\pi f$, ε_o represents the permittivity of free space, Tanδ represents the dissipation factor and ε' represents the dielectric constant.

Figure 5.20 shows the variation in AC conductivity with respect to frequency. It was observed that as the frequency increases AC conductivity increases. This trend can be explained based on Max-well Wagner two lattice model. At lower frequency grain boundaries are more active and provide resistance to the hopping mechanism of electrons which occur between Fe^{2+} and Fe^{3+},but at high frequency the conductive grain become more active and promotes the hopping mechanism of electrons [52]. When the copper and silver are doped into the nickel ferrites nanoparticles AC conductivity increases because both dopants have the conductive nature and they contribute towards the increase in conductivity.

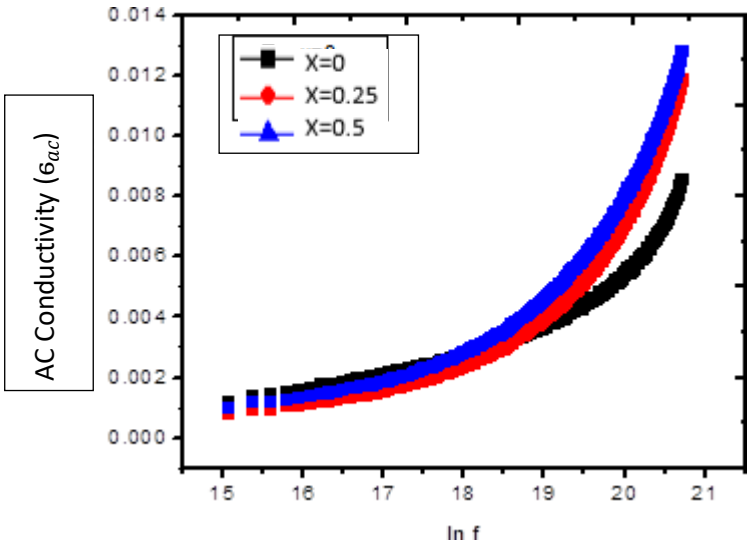

Figure 5. 17 AC conductivity of copper silver doped nickel ferrites nanoparticles

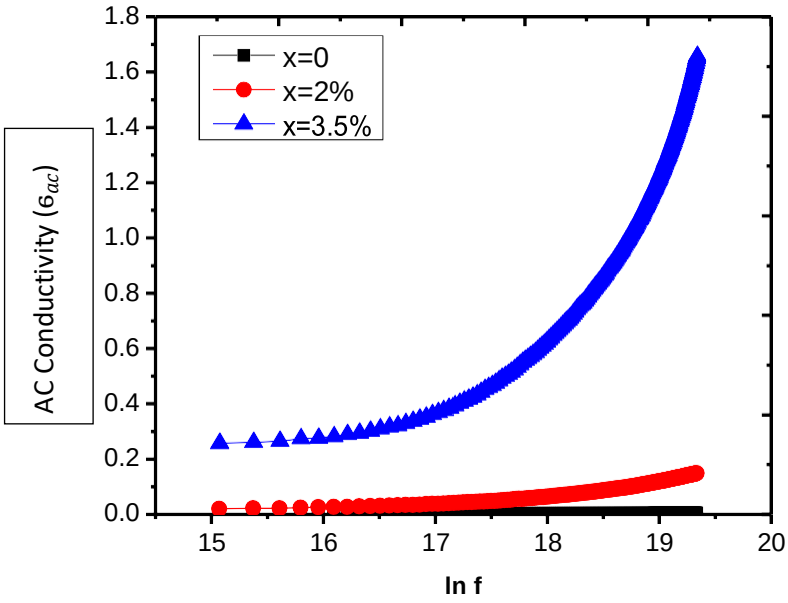

Figure 5. 18 AC conductivity of Ferrites and Graphene Nanocomposites

Figure 5.21 shows the AC conductivity of $Ni_{0.5}(CuAg)_{0.5}Fe_2O_4$ @Graphene where x= 2% and 3.5 %. The presence of graphene in nanocomposites further increases the conductivity. The band conduction and hopping conduction increases with the addition of graphene. On the grain boundaries graphene provides the continuous path for the fast and sustained transportation of electrons.

5.9 Impedance

Figure 5.23 shows the relation between impedance and frequency. It was observed that with the addition of the copper and silver the impedance decreases. Impedance is defined as the total resistance of the system. Conductive nature of dopants is responsible for the decrease in impedance values.

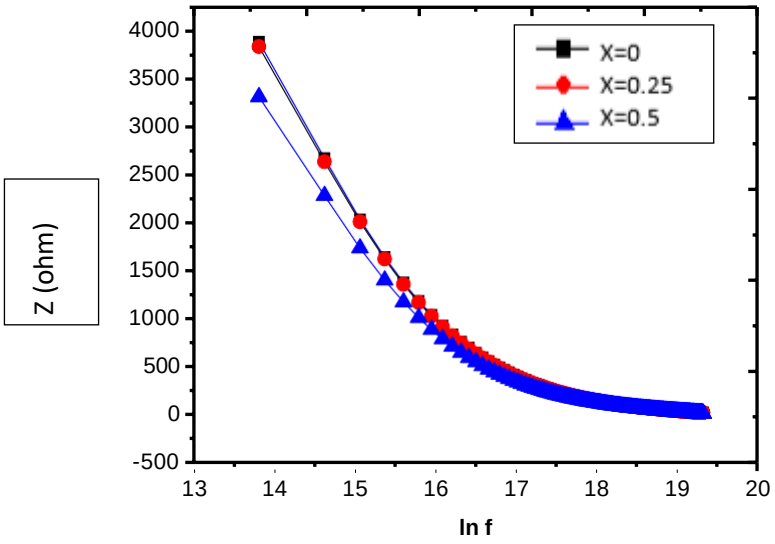

Figure 5. 19 Impedance of copper silver doped nickel ferrites nanoparticles

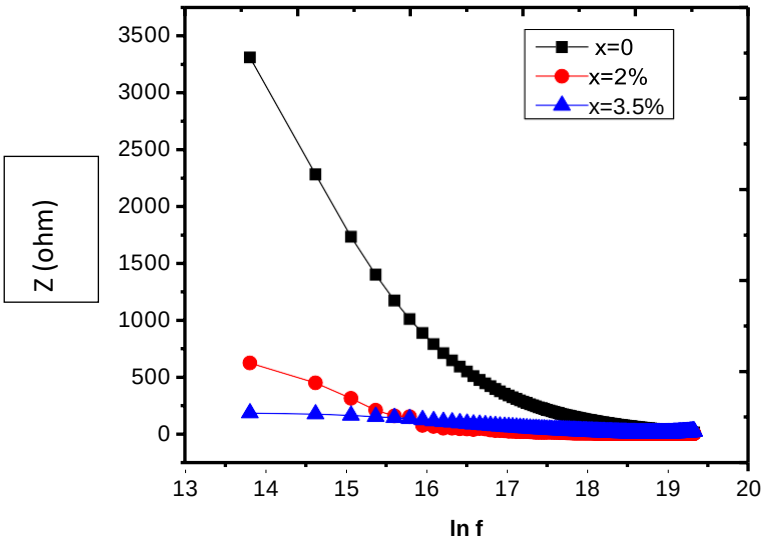

Figure 5. 20 Impedance of ferrites and graphene nanocomposites

Figure 5.23 shows the trend of impedance of $Ni_{0.5}(CuAg)_{0.5}Fe_2O_4$ @Graphene where x= 2% and 3.5 %. The decrease in impedance is observed due to the increased conductivity near the grain boundaries by adding graphene in nickel ferrite nanoparticles. The pi electrons of graphene responsible to reduce resistivity. The bonding and anti-bonding of the pi electrons of graphene dictated the electrical conductivity of graphene.

Table.5. 4 Dielectric constant at 1 MHz and 1 GHz

Samples	Dielectric Constant at 1 MHz	Dielectric Constant at 1 GHz
$NiFe_2O_4$	9.00	5.81
$Ni_{0.75}(CuAg)_{0.25}Fe_2O_4$	10.00	6.45
$Ni_{0.5}(CuAg)_{0.5}Fe_2O_4$	11.47	6.89
$Ni_{0.5}(CuAg)_{0.5}Fe_2O_4$+2% G	90.85	36.42
$Ni_{0.5}(CuAg)_{0.5}Fe_2O_4$+3.5%G	116.60	45.08

Table.5. 5.Dielectric loss and Ac conductivity of samples

Samples	Dielectric Loss at 1 MHz	AC conductivity At 1 MHz
$NiFe_2O_4$	3.88	0.008
$Ni_{0.75}(CuAg)_{0.25}Fe_2O_4$	4.89	0.011
$Ni_{0.5}(CuAg)_{0.5}Fe_2O_4$	5.92	0.013
$Ni_{0.5}(CuAg)_{0.5}Fe_2O_4$+2% G	103.31	0.1
$Ni_{0.5}(CuAg)_{0.5}Fe_2O_4$+3.5%G	416.00	1.7

Conclusions

The copper silver doped Nickel Ferrites nanoparticles $Ni_{1-x}(CuAg)_xFe_2O_4$,where x=0, 025 ,0.5 were successfully synthesized by using Co-precipitation route. XRD pattern of $Ni_{1-x}(CuAg)_xFe_2O_4$ confirm that all the prepared samples exhibit single cubic phase structure. There was no impurity observed in the prepared samples. Crystallite size was found using Scherer equation which lies within the range of 20 to 50 nm. Calculations from XRD patterns provide information regarding X-ray density, bulk density, lattice parameters and porosity of the samples. SEM images clearly show that prepared nanoparticles were fine, spherical in shape and there was no agglomeration observed. SEM images shows that particle size increases as the dopant is introduced into the system because of the large ionic radii of the dopants. FTIR analysis confirm the presence of metal -oxygen bonds in tetrahedral and octahedral sites of the ferrites and with the addition of dopants, bands are shifted towards the lower frequency which shows the redistribution of cations. The LCR meter was used to study the dielectric properties of prepared ferrites. Dielectric constant increases as the dopants are introduce into the system due to the conductive nature of dopants which increases the number of charge carriers. Dielectric constant and Dielectric loss of nickel ferrite is increases from 9.00 to 11.46 and 3.88 to 5.92 for doped nickel ferrites nanoparticles. AC conductivity increases from 0.001 to 9.66. All the properties like dielectric constant, dielectric loss, tangent loss, AC conductivity trends were in the good agreement with the Maxwell-Wagner model and Koop's theory.

$Ni_{0.5}(CuAg)_{0.5}Fe_2O_4$ @Graphene Nanocomposites were prepared by using dispersion method. $Ni_{0.5}(CuAg)_{0.5}Fe_2O_4$ was selected based on high dielectric properties and graphene was used to make nanocomposites with $Ni_{0.5}(CuAg)_{0.5}Fe_2O_4$ nanoparticles. 2% and 3.5% Graphene was used. Water was used as a dispersive medium. XRD of the nanocomposites shows no structural changes in the composites. SEM images of nanocomposites clearly show that ferrites nanoparticles were uniformly decorated along the graphene sheet. FTIR spectrum

of graphene show the band in the range of 1600 to 1800 cm^{-1} which indicate the c=c bond in graphene. The dielectric properties of nanocomposite show the huge enhancement in dielectric constant, dielectric loss, tangent loss and in AC conductivity due to the conductive nature of graphene which promotes the hopping mechanism of electrons and high surface area and porosity of graphene. Dielectric constant and Dielectric loss of doped nickel ferrites nanoparticles increases from 11.47 to 116.60 and 5.92 to 416 for nanocomposites. AC conductivity increases from 9.6 to 25 for nanocomposites.

Future Work

Regarding the study of ferrites there are various parameters that can be tuned to investigate the different properties of ferrites and their nanocomposites like electrical properties, optical properties, magnetic properties and dielectric properties.

- Beside the graphene different composites can be prepared with polymers, Single walled carbon nanotubes (SWCNT), Multi walled carbon nanotubes (MWCNTs) to study their effects.
- Different methods to prepare ferrites nanoparticles can be used and comparative study would be possible. Different dopants can be used to study their effects in different concentration.
- Synthesis parameters like pH and temperature can also be studied to investigate structural properties. The prepared Nano composites can be very useful in various industrial applications. Such as dielectric, microwave, electromagnetic, optical and magnetic applications.

References

[1] L. Thakur and B. Singh, "History and applications of important Ferrites," *Integrated Research Advances,* vol. 1, pp. 11-13, 2014.

[2] J. Haspers, "Ferrites: Their Properties and Applications," in *Modern Materials*. vol. 3, ed: Elsevier, 1962, pp. 259-341.

[3] V. Verma, J. Kapil, and N. Singh, "Structural, magnetic properties of soft and hard ferrites and their emi shielding application in X-band frequency range," *International Journal of Engineering Research & Technology (IJERT),* pp. 557-560, 2014.

[4] R. C. Pullar, "Hexagonal ferrites: a review of the synthesis, properties and applications of hexaferrite ceramics," *Progress in Materials Science,* vol. 57, pp. 1191-1334, 2012.

[5] D. S. Mathew and R.-S. Juang, "An overview of the structure and magnetism of spinel ferrite nanoparticles and their synthesis in microemulsions," *Chemical engineering journal,* vol. 129, pp. 51-65, 2007.

[6] N. Gupta, P. Jain, R. Rana, and S. Shrivastava, "Current development in synthesis and characterization of nickel ferrite nanoparticle," *Materials Today: Proceedings,* vol. 4, pp. 342- 349, 2017.

[7] G. Nabiyouni, M. J. Fesharaki, M. Mozafari, and J. Amighian, "Characterization and magnetic properties of nickel ferrite nanoparticles prepared by ball milling technique," *Chinese Physics Letters,* vol. 27, p. 126401, 2010.

[8] R. Valenzuela, "Novel applications of ferrites," *Physics Research International,* vol. 2012, 2012.

[9] R. Mas-Balleste, C. Gomez-Navarro, J. Gomez-Herrero, and F. Zamora, "2D materials: to graphene and beyond," *Nanoscale,* vol. 3, pp. 20-30, 2011.

[10] D. Li and R. B. Kaner, "Graphene-based materials," *Nat Nanotechnol,* vol. 3, p. 101, 2008.

[11] D.-H. Chen and X.-R. He, "Synthesis of nickel ferrite nanoparticles by sol-gel method," *Materials Research Bulletin,* vol. 36, pp. 1369-1377, 2001.

[12] Y. Liu, X. X. Liu, and Z. Y. Zhang, "Preparation and Microwave Absorption Property of Nickel Spinel Ferrite," in *Key Engineering Materials*, 2013, pp. 36-39.

[13] P. A. Noorkhan and S. Kalayne, "Synthesis, Characterization Ac Conductivity of Nickel Ferrite," *Journal of Engineering Research and Applications,* vol. 2, pp. 681-685, 2012.

[14] V. V. Dhole, "INTERNATIONAL JOURNAL OF ENGINEERING SCIENCES & RESEARCH TECHNOLOGY STRUCTURAL AND MAGNETIC PROPERTIES OF NICKEL FERRITE NANOPARTICLES BY WET CHEMICAL CO-PRECIPITATION TECHNIQUE."

[15] S. Anjum, A. Rashid, F. Bashir, S. Riaz, M. Pervaiz, and R. Zia, "Effect of Cu-doped nickel ferrites on structural, magnetic, and dielectric properties," *IEEE Transactions on Magnetics,* vol. 50, pp. 1-4, 2014.

[16] K. V. Babu, G. Satyanarayana, B. Sailaja, G. S. Kumar, K. Jalaiah, and M. Ravi, "Structural and magnetic properties of Ni0. 8M0. 2Fe2O4 (M= Cu, Co) nano-crystalline ferrites," *Results in Physics,* vol. 9, pp. 55-62, 2018.

[17] P. Yin, Y. Deng, L. Zhang, W. Wu, J. Wang, X. Feng, *et al.*, "One-step hydrothermal synthesis and enhanced microwave absorption properties of Ni0. 5Co0. 5Fe2O4/graphene composites in low frequency band," *Ceramics International,* vol. 44, pp. 20896-20905, 2018.

[18] S. A. Soomro, I. H. Gul, M. Z. Khan, H. Naseer, and A. N. Khan, "Dielectric properties evaluation of NiFe2O4/MWCNTs nanohybrid for microwave applications prepared via novel one step synthesis," *Ceramics International,* vol. 43, pp. 4090-4095, 2017.

[19] S. Akhter, D. P. Paul, M. A. Hakim, D. K. Saha, M. Al-Mamun, and A. Parveen, "Synthesis, structural and physical properties of Cu1–xZnxFe2O4 ferrites," *Materials Sciences and Applications,* vol. 2, p. 1675, 2011.

[20] L. Zhang, X. Yu, H. Hu, Y. Li, M. Wu, Z. Wang, *et al.*, "Facile synthesis of iron oxides/reduced graphene oxide composites: application for electromagnetic wave absorption at high temperature," *Scientific reports,* vol. 5, p. 9298, 2015.

[21] R. Singh, J. Ladol, H. Khajuria, and H. N. Sheikh, "Nitrogen doped graphene nickel ferrite magnetic photocatalyst for the visible light degradation of methylene blue," *Acta Chimica Slovenica,* vol. 64, pp. 170-178, 2017.

[22] A. Teber, K. Cil, T. Yilmaz, B. Eraslan, D. Uysal, G. Surucu, *et al.*, "Manganese and zinc spinel ferrites blended with multi-walled carbon nanotubes as microwave absorbing materials," *Aerospace,* vol. 4, p. 2, 2017.

[23] X. Zhao, Z. Zhang, L. Wang, K. Xi, Q. Cao, D. Wang, *et al.*, "Excellent microwave absorption property of graphene-coated Fe nanocomposites," *Scientific reports,* vol. 3, p. 3421, 2013.

[24] J. Balavijayalakshmi, N. Suriyanarayanan, and R. Jayaprakash, "Role of copper on structural, magnetic and dielectric properties of nickel ferrite nano particles," *Journal*

of Magnetism and Magnetic Materials, vol. 385, pp. 302-307, 2015.

[25] E. R. Kumar, R. Jayaprakash, G. S. Devi, and P. S. P. Reddy, "Magnetic, dielectric and sensing properties of manganese substituted copper ferrite nanoparticles," *Journal of Magnetism and Magnetic Materials,* vol. 355, pp. 87-92, 2014.

[26] Z. Wang and Z. Guang-Lin, "Microwave absorption properties of carbon nanotubes-epoxy composites in a frequency range of 2-20 GHz," *Open Journal of Composite Materials,* vol. 3, p. 17, 2013.

[27] J. Fang, W. Zha, M. Kang, S. Lu, L. Cui, and S. Li, "Microwave absorption response of nickel/graphene nanocomposites prepared by electrodeposition," *Journal of materials science,* vol. 48, pp. 8060-8067, 2013.

[28] X. Yuan, B. Liu, H. Hou, K. Zeinu, Y. He, X. Yang, *et al.*, "Facile synthesis of mesoporous graphene platelets with in situ nitrogen and sulfur doping for lithium–sulfur batteries," *Rsc Advances,* vol. 7, pp. 22567-22577, 2017.

[29] R. Ahmad, I. H. Gul, M. Zarrar, H. Anwar, M. B. khan Niazi, and A. Khan, "Improved electrical properties of cadmium substituted cobalt ferrites nano-particles for microwave application," *Journal of Magnetism and Magnetic Materials,* vol. 405, pp. 28-35, 2016.

[30] O. A. Al-Hartomy, A. A. Al-Ghamdi, F. Al-Salamy, N. Dishovsky, R. Shtarkova, V. Iliev, *et al.*, "Dielectric and microwave properties of graphene nanoplatelets/carbon black filled natural rubber composites," *International Journal of Materials and Chemistry,* vol. 2, pp. 116-122, 2012.

[31] R. S. Alam, M. Moradi, and H. Nikmanesh, "Influence of multi-walled carbon nanotubes (MWCNTs) volume percentage on the magnetic and microwave absorbing properties of BaMg

0.5 Co 0.5 TiFe 10 O 19/MWCNTs nanocomposites," *Materials Research Bulletin,* vol. 73, pp. 261-267, 2016.

[32] D. Kumar, K. Singh, V. Verma, and H. Bhatti, "Microwave assisted synthesis and characterization of graphene nanoplatelets," *Applied Nanoscience,* vol. 6, pp. 97-103, 2016.

[33] X. Zhang, X. Sun, Y. Chen, D. Zhang, and Y. Ma, "One-step solvothermal synthesis of graphene/Mn 3 O 4 nanocomposites and their electrochemical properties for supercapacitors," *Materials Letters,* vol. 68, pp. 336-339, 2012.

[34] Z. Durmus, A. Durmus, and H. Kavas, "Synthesis and characterization of structural and magnetic properties of graphene/hard ferrite nanocomposites as microwave-absorbing

material," *Journal of Materials Science,* vol. 50, pp. 1201-1213, 2015.

[35] J. Ai, E. Biazar, M. Jafarpour, M. Montazeri, A. Majdi, S. Aminifard, *et al.*, "Nanotoxicology and nanoparticle safety in biomedical designs," *Int J Nanomedicine,* vol. 6, pp. 1117-1127, 2011.

[36] C. Murugesan, M. Perumal, and G. Chandrasekaran, "Structural, dielectric and magnetic properties of cobalt ferrite prepared using auto combustion and ceramic route," *Physica B: Condensed Matter,* vol. 448, pp. 53-56, 2014.

[37] P. Iqbal, J. A. Preece, and P. M. Mendes, "Nanotechnology: The "Top-Down" and "Bottom-Up" Approaches," *Supramolecular Chemistry: From Molecules to Nanomaterials,* 2012.

[38] D. Mijatovic, J. C. Eijkel, and A. van den Berg, "Technologies for nanofluidic systems: top-down vs. bottom-up—a review," *Lab on a Chip,* vol. 5, pp. 492-500, 2005.

[39] S. S. Su and I. Chang, "Review of Production Routes of Nanomaterials," in *Commercialization of Nanotechnologies–A Case Study Approach*, ed: Springer, 2018, pp. 15-29.

[40] A. Rajaeiyan and M. Bagheri-Mohagheghi, "Comparison of sol-gel and co-precipitation methods on the structural properties and phase transformation of γ and α-Al 2 O 3 nanoparticles," *Advances in Manufacturing,* vol. 1, pp. 176-182, 2013.

[41] D. Cui, J. Wang, A. Sun, H. Song, and W. Wei, "Anomalously Faster Deterioration of LiNi0. 8Co0. 15Al0. 05O2/Graphite High-Energy 18650 Cells at 1.5 C than 2.0 C," *Scanning,* vol. 2018, 2018.

[42] R. Sharma, D. Bisen, U. Shukla, and B. Sharma, "X-ray diffraction: a powerful method of characterizing nanomaterials," *Recent research in science and technology,* vol. 4, 2012.

[43] R. Melo, F. Silva, K. Moura, A. de Menezes, and F. Sinfrônio, "Magnetic ferrites synthesised using the microwave-hydrothermal method," *Journal of Magnetism and Magnetic Materials,* vol. 381, pp. 109-115, 2015.

[44] J. Ai, E. Biazar, M. Jafarpour, M. Montazeri, A. Majdi, S. Aminifard, *et al.*, "Nanotoxicology and nanoparticle safety in biomedical designs," *International journal of nanomedicine,* vol. 6, p. 1117, 2011.

[45] Z. G. Özdemir, N. Y. Canli, B. Senkal, Y. Gürsel, and M. Okutan, "Super-capacitive behavior of carbon nano tube doped 11-(4-cyanobiphenyl-4-oxy) undecan-1-ol," *Journal of Molecular Liquids,* vol. 211, pp. 442-447, 2015.

[46] A. A. Ali, M. Eltabey, B. M. Abdelbary, and S. H. Zoalfakar, "MWCNTs/carbon nano fibril composite papers for fuel cell and super capacitor applications," *Journal of*

Electrostatics, vol. 73, pp. 12-18, 2015.

[47] S. Sagadevan, Z. Z. Chowdhury, and R. F. Rafique, "Preparation and Characterization of Nickel ferrite Nanoparticles via Co-precipitation Method," *Materials Research*, vol. 21, 2018.

[48] M. Siyar, N. Khan, A. Maqsood, M. Younas, and M. Daud, "Structural Properties and Mechanical Characterizations of Graphene Based Cobalt-ferrites Nanocomposites for Load Baring Applications."

[49] M. Ajmal and A. Maqsood, "Structural, electrical and magnetic properties of Cu1−xZnxFe2O4 ferrites (0≤ x≤ 1)," *Journal of Alloys and Compounds*, vol. 460, pp. 54-59, 2008.

[50] S. Mahalakshmi, K. S. Manja, and S. Nithiyanantham, "Structural and morphological studies of copper-doped nickel ferrite," *Journal of Superconductivity and Novel Magnetism*, vol. 28, pp. 3093-3098, 2015.

[51] C. Koops, "On the dispersion of resistivity and dielectric constant of some semiconductors at audiofrequencies," *Physical Review*, vol. 83, p. 121, 1951.

[52] M. Anis-ur-Rehman, M. Malik, S. Nasir, M. Mubeen, K. Khan, and A. Maqsood, "Structural, electrical and dielectric properties of nanocrystalline Mg-Zn ferrites," in *Key Engineering Materials*, 2012, pp. 51-57.